Journal of Paleontology, 90(4), 2016, p. 741–762
Copyright © 2016, The Paleontological Society
0022-3360/16/0088-0906
doi: 10.1017/jpa.2016.64

Journal of PALEONTOLOGY
A JOURNAL OF THE PALEONTOLOGICAL SOCIETY

Scanning electron microscope examination of the dental enameloid of the Cretaceous durophagous shark *Ptychodus* supports neoselachian classification

Brian L. Hoffman, Scott A. Hageman, and Gregory D. Claycomb

Department of Natural and Applied Sciences, Park University, Parkville, Missouri 64152, USA ⟨brian.hoffman@park.edu⟩, ⟨shageman@park.edu⟩, ⟨gclaycomb@park.edu⟩

Abstract.—Although *Ptychodus* teeth are well known in Late Cretaceous marine deposits in North America and Europe and a few specimens with jaw elements have been discovered, the taxonomic position of the shark genus *Ptychodus* is enigmatic due to the lack of preservation of diagnostic material other than teeth. These sharks possessed a pavement dentition suited to a diet of hard-shelled macroinvertebrates (durophagy), leading several studies to variously describe *Ptychodus* as a batoid, a hybodont shark, or a selachimorph. Members of the Selachimorpha share one dental synapomorphy, a triple-layered enameloid (TLE) consisting of an outer shiny-layered enameloid (SLE) of randomly oriented hydroxyapatite crystallites, a middle layer of parallel-bundled enameloid (PBE), and an inner layer of tangled-bundled enameloid (TBE). Batoids and hybodonts both have teeth with single crystallite enameloid (SCE). We examined teeth from *Ptychodus* collected from the Lincoln Limestone of the Greenhorn Formation of Barton County, Kansas, and compared their enameloid ultrastructure with that of a Carboniferous hybodontiform and the Cretaceous lamniform shark *Squalicorax curvatus* Williston, 1900. Scanning electron microscopic examination of *Ptychodus* shows that crystallite bundling in the form of a TLE is evident in these teeth. The PBE is most apparent at transverse enameloid ridges of *Ptychodus* teeth. Columns of dentine penetrate into the tooth enameloid, and the crystallites near the dentine are randomly oriented. These observations bolster the argument that *Ptychodus* is a genus of highly specialized selachimorph shark, rather than a hybodont or batoid.

Introduction

The study of fossil sharks is often difficult due to lack of preservation of mostly cartilaginous skeletal elements. The most durable material for study is teeth and scales, and sampling bias generally means that only the most complete and largest specimens are studied in great detail (Cappetta, 2012). Other elements, such as body outlines, fin spines, vertebral centra, and other skeletal elements are rarely available for study. Morphological and molecular studies of extant sharks indicate that the neoselachians are monophyletic (e.g., Douady et al., 2003; Winchell et al., 2004; Rocco et al., 2007; Cappetta, 2012). Numerous neoselachian skeletal synapomorphies exist, which are usually not instructive when dealing with incomplete fossil shark specimens. As for neoselachian dental material, one dental synapomorphy has been cited—a triple-layered enameloid (TLE; Reif, 1973)—making this feature a key marker of neoselachian descent.

Paleozoic sharks (including symmoriids, ctenacanths, and hybodonts) typically have a dental enameloid composed of randomly oriented fluoroapatite crystallites called single crystallite enameloid (SCE; Ginter et al., 2010; Cappetta, 2012). Reif (1973) described neoselachian enameloid as being composed of three layers of fluoroapatite crystal fibers (Fig. 1): a superficial shiny-layered enameloid (SLE), which is homologous to the SCE of primitive sharks (Andreev and Cuny, 2012); an intermediate parallel-bundled enameloid (PBE); and a deep tangled-bundled enameloid (TBE). The parallel-oriented bundles of crystallites follow three directions (Fig. 1): (1) axial fibers run parallel to the baso-apical axis of the tooth; (2) radial bundles run from enameloid to the dentine and lie orthogonal to the axial fibers; and (3) circumferential fibers run just under the SCE around the tooth crown. The PBE layer gradually transitions to a layer of haphazardly organized fiber bundles (TBE), which in turn transition to single crystallites at the enameloid-dentine junction (EDJ). Enault et al. (2015) proposed eliminating the term ‘SLE’ and naming the outer single crystallite layer of the triple-layered enameloid ‘SCE.’ Some authors consider the PBE + TBE to be a single bundled layer (Cuny and Risnes, 2005; Enault et al., 2015) with the defining part of this structure being the parallel-bundled fibers (Maisey et al., 2004; Cuny and Risnes, 2005). Several studies have shown that batoid teeth have either an SCE or double-layered enameloid (e.g., Preuschoft et al., 1974; Reif, 1977; Maisey et al., 2004; Cuny et al., 2009; Enault et al., 2013). This observation, coupled with phylogenetics demonstrating the monophyly of the batoids and the position of the batoids as a sister group to modern sharks (e.g., Douady et al., 2003; Winchell et al., 2004; Rocco et al., 2007) indicates that TLE is likely a synapomorphy of the selachimorphs and not neoselachians as a whole (Enault et al., 2013). In terms of function, the SCE/SLE is thought to provide resistance to cracking

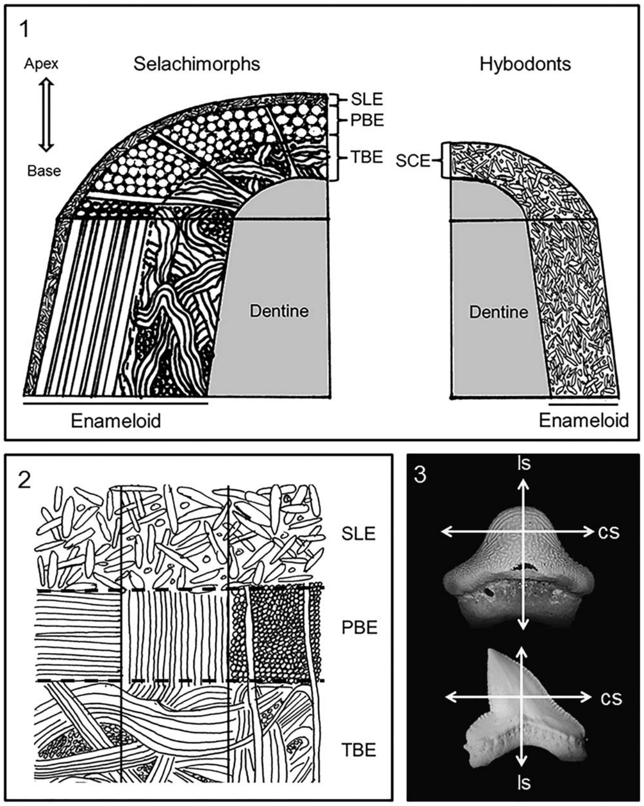

Figure 1. Schematic representation of neoselachian triple-layered enameloid. (**1**) Enameloid of selachimorph sharks (left) and hybodonts (right) in cross section (top surface) and longitudinal section (front surface). The layers are shiny-layered enameloid (SLE), parallel-bundled enameloid (PBE), tangled-bundled enameloid (TBE), and single-crystallite enameloid (SCE). (**2**) The PBE of selachimorph sharks may appear to have three basic orientations, depending on tooth section. The bundles may appear to run parallel to the tooth surface (left), perpendicular to the tooth surface (middle), or perpendicular to the tooth surface and cut edgewise (right). The SLE and SCE, which contain single enameloid crystallites and TBE, have the same pattern regardless of orientation because of the random nature of crystallite and bundle distribution. (**3**) Planes of section described in this study: cross section (cs) and longitudinal section (ls) in *Ptychodus* (top) and *Squalicorax* (bottom). No size relationship is implied by the schematic.

of the enameloid (Reif, 1977); PBE resists bending force; and the TBE resists compressional stresses (Preuschoft et al., 1974; Whitenack et al., 2011), although this has proven difficult to demonstrate in nanoindentation experiments (Whitenack et al., 2010; Enax et al., 2014).

Although isolated *Ptychodus* teeth are relatively common and many associated and even articulated dental sets are known, skeletal material for this genus is rare. Round, calcified vertebral centra have been discovered with associated tooth sets, as have denticles, jaw elements, and pieces of neurocranium. The presence of calcified vertebral centra, a neoselachian autapomorphy, leads many researchers to classify *Ptychodus* as a specialized neoselachian (e.g., Stewart, 1980; Everhart and Caggiano, 2004). A competing hypothesis is that *Ptychodus* is a hybodont shark because of similarities in tooth morphology, including the anaulacorhizous root and enameloid that has been described as an SCE in *Ptychodus* sp. from France (e.g., Cuny, 2008; Cappetta, 2012; Enault et al., 2015). In this study, we examined the enameloid in whole and sectioned teeth of *Ptychodus* using scanning electron microscopy and report here the occurrence of the TLE structure in these species, confirming findings previously available only in the one relatively obscure publication (Bendix-Almgreen, 1983, fig. 6a, 6b) and the so-called gray literature (David, 1996, 1999). *Ptychodus* enameloid structure was compared to that of *Squalicorax curvatus* Williston, 1900 (Elasmobranchii: Neoselachii) and an indeterminate Upper Pennsylvanian hybodontiform. The presence of TLE in *Ptychodus* argues for the neoselachian classification of the genus.

Materials and methods

The ultrastructure of the enameloid in isolated chondrichthyan teeth was studied by well-known methods (e.g., Bendix-Almgreen, 1983; Gillis and Donoghue, 2007; Guinot and Cappetta, 2011). Whole teeth or sectioned teeth were etched in 10% hydrochloric acid (HCl; Fisher Chemical) for the length of time required to achieve the desired degree of relief, usually 5 seconds to 3 minutes. The single crystallite structure of the SLE is very susceptible to acid etching and 30- to 60-second exposures to acid will permit its observation. The PBE and TBE layers are much more resistant to acid etching and require etching times of two to five minutes. Some teeth were sectioned by embedding them in clear polyester resin then grinding them by hand to the desired level using a series of sandpapers. The embedded specimens were wet ground first with 400-grit sandpaper (3M Wetordry), followed by 600-, 1,000-, 1,500-, 2,000-, and 3,000-grit papers. Relief was generated in the ground specimens by acid etching with 10% HCl for five to ten seconds. Following acid etching, samples were coated with gold using a Cressington 108auto sputter coater and visualized using a JEOL JSM-5900 scanning electron microscope. For identification purposes, the appearance of ridges and tubercles in the enameloid was enhanced prior to light photography by coating the teeth with sublimated ammonium chloride (Fisher Chemical).

The specimens (with the exception of the hybodontiform) utilized for this study were collected by the late Alan H. Kamb, longtime assistant curator of the Invertebrate Paleontology Museum at the University of Kansas, over a period of several years from the Lincoln Limestone Member of the Greenhorn Limestone Formation near Hoisington, Barton County, Kansas. The Kamb family donated much of Mr. Kamb's personal collection to Park University following his death in 1998. The *Squalicorax* teeth were labeled '*Corax* sp.' and the *Ptychodus* teeth were designated '*Ptychodus* sp.' The Lincoln Limestone Member has been dated to the upper Cenomanian age (Kauffman et al., 1993; Gallardo et al., 2013).

Teeth of a Pennsylvanian hybodontiform were collected by 10% acetic acid maceration of blocks of limestone and sequential sifting of the acid insoluble residue using 10-, 20- and 40-mesh brass sieves. After rinsing with deionized water and air drying, fossils were picked from the graded sediment with the aid of a dissecting stereomicroscope. Samples were obtained from the Farley Limestone Member, Lane Formation, Kansas City Group, Missourian Stage (Kasimovian), Upper Pennsylvanian, Carboniferous Period on the campus of Park University, Parkville, Platte County, Missouri (39.1882579°N, 94.678722°W).

Repositories and institutional abbreviations.—Figured and described material are indicated by the following acronyms: KUVP = Kansas University Museum of Natural History, Lawrence, Kansas; PUPC = Park University Department of Natural and Physical Sciences Paleontology Collection, Parkville, Missouri; PKUM = Geological Museum, Peking University, Beijing, China.

Systematic paleontology

Class Chondrichthyes Huxley, 1880
Subclass Elasmobranchii Bonaparte, 1838
Cohort Euselachii Hay, 1902
Order Hybodontiformes Maisey, 1975
Gen. indet. sp. indet.
Figures 2.1–2.11, 4.1–4.6

Material.—Two relatively complete, albeit broken teeth (Fig. 2.1–2.5), several tooth fragments, a fragment of hybodontiform dorsal fin spine (Fig. 2.6) and nine denticles.

Description.—The most complete tooth (Fig. 2.1–2.5) resembles those of *Onychoselache traquari* Dick, 1978 and has a similar morphology to that of a specimen identified as *Onychoselache* sp. in Ginter et al. (2010, fig. 92D) from the Mississippian (Tournaisian) of Muhua, Southern China (PKUM unnumbered). The tooth shape is rectangular, and the crown is not greatly offset from the anaulacorhizous root, which is penetrated by several expanded foramina opening into channels in the root. The root makes up about 70% of the entire height of the tooth. The crown is relatively flat, likely forming a grinding dentition, with a median occlusal crest. The crowns of these teeth are colored black, while the root is beige.

We recovered other hybodontiform ichthyoliths with these teeth and tooth fragments. One piece of dorsal fin spine was found during our study (Fig. 2.6). This 1 mm fragment has two posterior denticles, each of which resembles hybodontiform denticles found with the teeth and fin spine fragment. A line of secondary fusion of the denticles with the spine is in evidence, as in several hybodont sharks. Unique hooked denticles resembling those described lining the pectoral fin and lateral line in *Onychoselache traquari* (Dick and Maisey, 1980; Coates and Gess, 2007) are also present with these teeth. Four of these denticles match descriptions of those that line the edge of the pectoral fin, having rounded bases and smooth cusps that point mesially toward the fin insertion (Fig. 2.7–2.9). The three putative lateral line denticles have a thin, subtriangular base (Fig 2.10, 2.11).

Remarks.—Hybodonts were primarily Mesozoic sharks, although stem hybodontiforms are known from the Paleozoic, perhaps as early as the Middle Devonian (Zangerl, 1981). Most Paleozoic hybodontids are known only from fragmentary remains, and several specimens of indeterminate hybodontiform sharks have been recovered from Pennsylvanian sediments of the Midcontinent Region (Hansen, 1986; Schultze and Chorn, 1988). The fragmentary nature of the isolated remains gathered for this study precludes further classification. Abundant prey for a durophagous predator in the form of gastropods, bivalves, and brachiopods (McKirahan et al., 2000) were discovered with these remains. The pectoral fins of some stem hybodontiforms such as *Onychoselache traquairi* are large and plesodic (Coates and Gess, 2007), providing the ability to hold an individual upright on a shallow sea bottom. This ability would have been advantageous to a similar shark in the shallow water and high wave energy of the Farley paleoenvironment, as evidenced by abundant ooids and polished specimens. The presence of amphibian skeletal remains (unpublished data, Hoffman, 2015) indicates that the Farley Limestone outcrop at Park University is composed of nearshore sediments.

Subcohort Neoselachii Compagno, 1977
Order *incertae sedis*
Family Ptychodontidae Jaekel, 1898
Genus *Ptychodus* Agassiz, 1835

Type species.—*Ptychodus mammillaris* Agassiz, 1839; Upper Cretaceous of Europe, no precise locality specified.

Remarks.—These teeth have massive crowns that are square to rectangular in shape and are decorated with a variety of transverse ridges, tubercles, and pits. The crown overhangs the anaulacorhizous root on all sides and the roots may be weakly bilobed. A durophagous lifestyle for these chondrichthyans is indicated by teeth that form a pavement dentition and attritional wear on the tooth crowns (e.g., Morton, 1834; Kauffman, 1972; Stewart, 1988; David, 1999; Hamm, 2008; Cappetta, 2012).

Ptychodus sp.

Figures 3.1–3.9; 7.1–7.6; 8.1–8.6; 9.1–9.6; 10.1–10.6; 11.1–11.6; 12.1–12.4; 13.1–13.6; 14.1–14.10

Material.—132 complete teeth; seven were surface etched with acid and 12 were sectioned prior to acid etching.

Description.—The teeth are relatively small for genus *Ptychodus*. The largest of these teeth measure 13 mm in width. The teeth have six to 15 subparallel transverse ridges that may bifurcate near the margin of the tooth. The marginal area is not well defined and is decorated with tubercles and ridges. The anterior face of the crown may be decorated with tubercles or ridges that are parallel to the labial-lingual axis and bifurcate near the labial margin. A well-developed concave notch is present on the lingual side of the crown, accommodating the labial shelf forming an articulation with the following tooth in the series. The crowns overhang the root on all sides. The roots tend to be weakly bilobate and anaulacorhizous, with nutrient foramina well evidenced on the labial side of the teeth near the root-crown border.

Remarks.—Due to heterodonty and intraspecific variation, it is often difficult to establish the identity of individual teeth of *Ptychodus*. There seems to be at least two species of *Ptychodus* represented in our collection. Most of the teeth appear to fall within the range of characters exhibited by *P. anonymus* Williston, 1900 (Fig. 3.1–3.6). These teeth have a high, rounded cusp with six to 15 transverse ridges. The transverse enameloid ridges tend to increase in concavity as the lingual side of the tooth is approached. The decoration in the marginal zone ranges

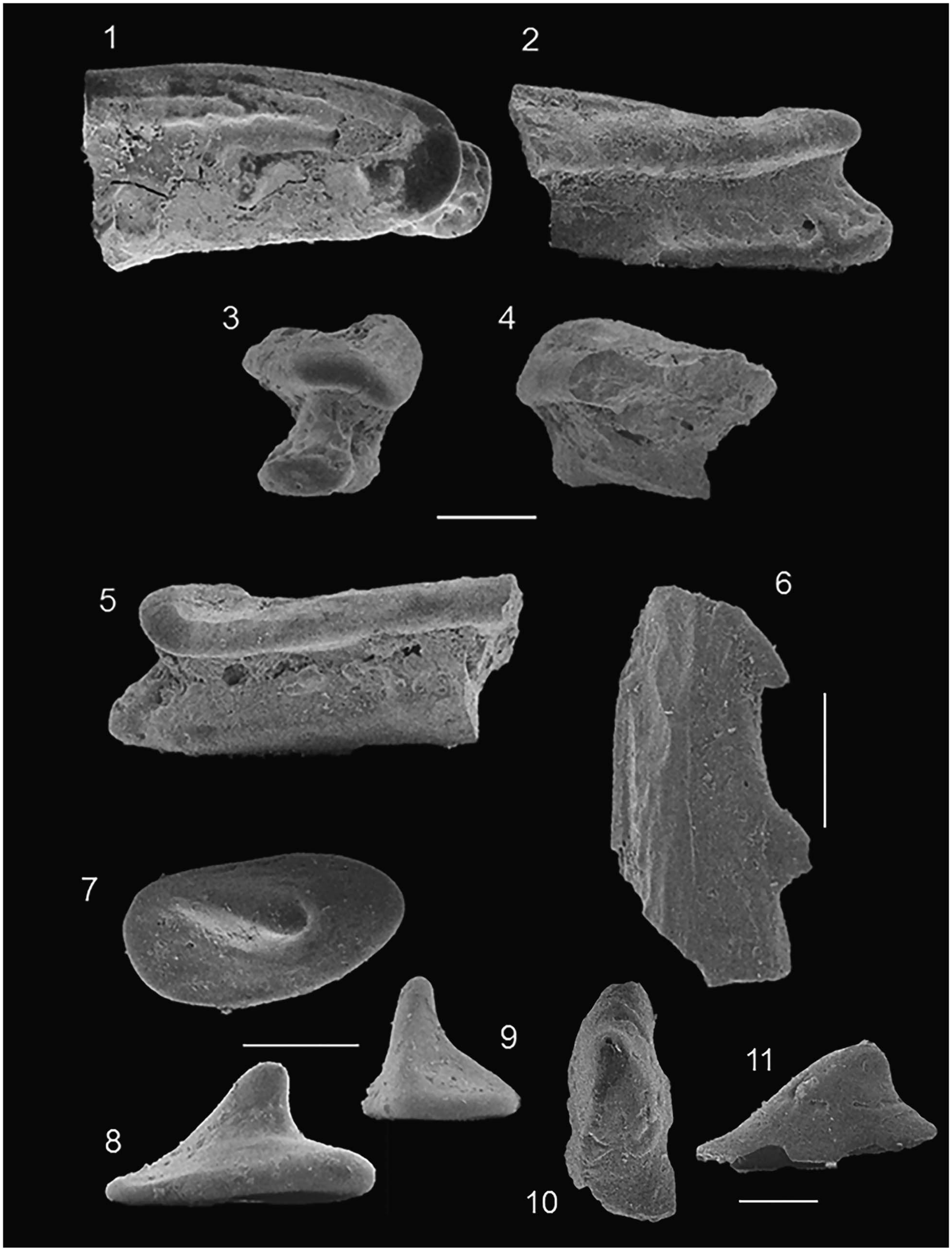

Figure 2. Ichthyoliths from indeterminate hybodontiform sharks from the Farley Member, Lane Formation, Kansas City Group, Upper Pennsylvanian (Kasimovian), Parkville, Platte County, Missouri, USA. Scanning electron micrographs: (**1–4**) Tooth fragment (PUPC 2015.02.01): (**1**) occlusal view; (**2**) lingual view; (**3, 4**) lateral views. (**5**) Labial view and (**6**) left lateral view of hybodontiform dorsal fin spine fragment, showing two posterior denticles (right). (**7–9**) Denticle presumably from pectoral fins: (**7**) apical view; (**8**) medial lateral view; (**9**) anterior view. (**10, 11**) Lateral line denticle: (**10**) apical view; (**11**) lateral view. (**1–5**) Scale bar = 1 mm; (**6–9**) scale bars = 500 µm; (**10, 11**) scale bar = 200 µm.

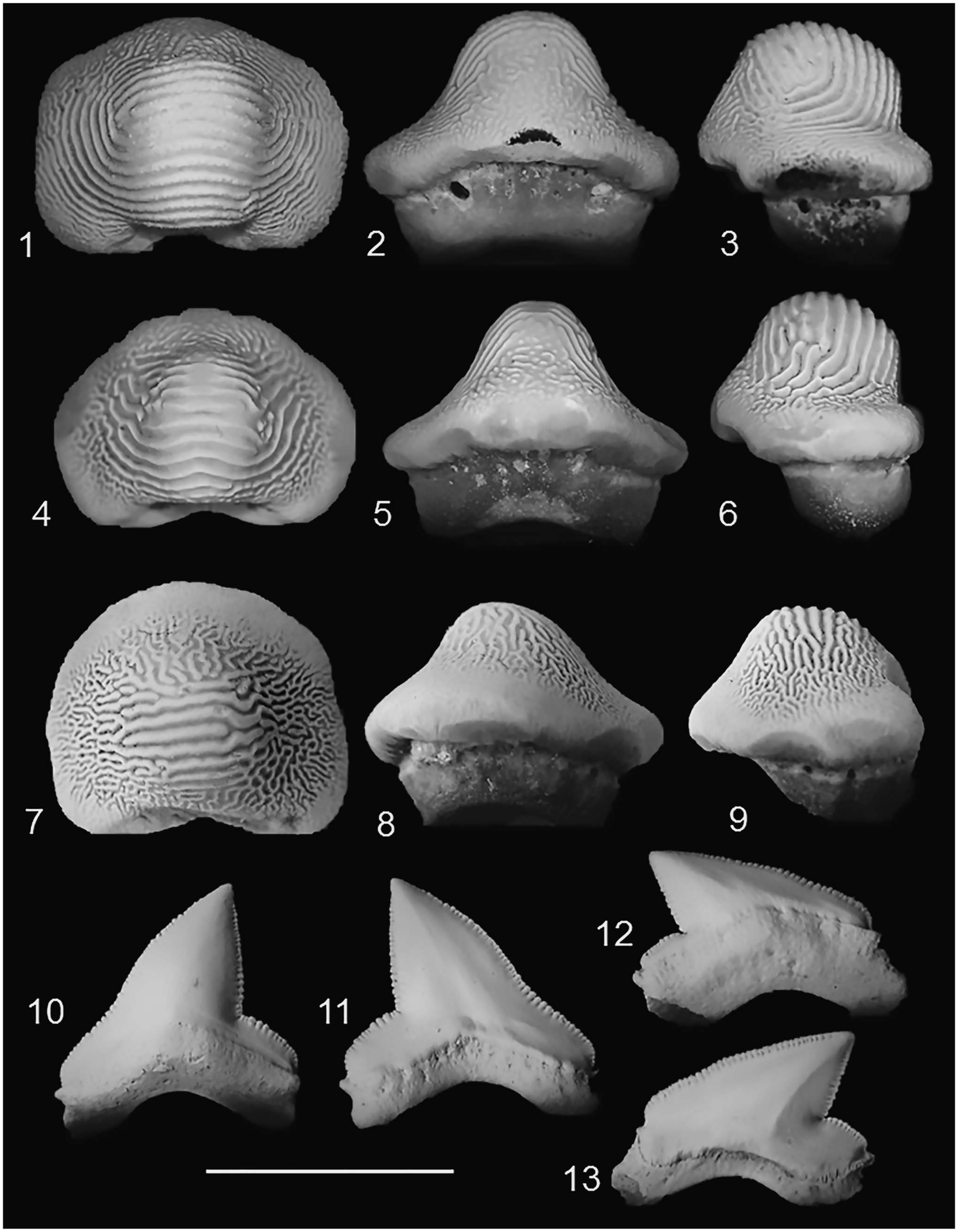

Figure 3. Teeth of *Ptychodus* sp. and *Squalicorax curvatus* from the Lincoln Limestone Member, Greenhorn Formation, Late Cretaceous (Cenomanian), Barton County, Kansas. Photomicrographs, all specimens dusted with ammonium chloride: (**1–9**) *Ptychodus* sp.; (**10–13**) *Squalicorax curvatus*; (**1–3**) PUPC 2015.03.03; (**4–6**) PUPC 2015.03.01; (**7–9**) PUPC 2015.03.02; (**10, 11**) PUPC 2015.04.1; (**12, 13**) PUPC 2015.04.02. (**1, 4, 7**) Occlusal views; (**2, 5, 8, 11, 13**) labial views; (**10, 12**) lingual views; (**3, 6, 9**) lateral views. Scale bar = 1 cm.

from being granular in appearance to a series of concentric ridges that are continuations of transverse ridges on the crown. The least abundant type of these teeth resembles *P. occidentalis* Leidy, 1868 (Fig. 3.7–3.9) and is square to rectangular in profile, with a rounded crown. Specimens have seven to 10 transverse ridges that begin to bifurcate on the crown and continue to anastomose into the marginal area.

Order Lamniformes Berg, 1937
Family Anacoracidae Casier, 1947
Genus *Squalicorax* Whitley, 1939

Type species.—*Corax pristodontus*, Agassiz, 1835; Maastrichtian, Maastricht, The Netherlands.

Squalicorax curvatus (Williston, 1900)
Figures 3.10–3.13; 5.1–5.6; 6.1–6.6

Material.—185 complete teeth, six of which were surface-etched with acid; five of the teeth were sectioned and then acid etched for this study.

Description.—All teeth have a distally inclined triangular cusp. The labial face of the crown is flat, and the lingual crown face is concave. The cutting edges of the crown are serrated. The mesial cutting edge is relatively long and straight or slightly convex. The distal cutting edge is shorter and convex. A serrated distal blade meets the base of the distal cutting edge of the main cusp at an acute angle, although this angle may be obtuse in anterior teeth. The largest teeth in this collection are 13 mm wide and 12 mm high. Lateral and posterior teeth tend to be lower in profile.

Remarks.—The taxonomy of the genus *Squalicorax* is in disarray, especially in regard to the '*S. falcatus* group' of the Western Interior Seaway of North America (Cumbaa et al., 2006). *S. falcatus* (Agassiz, 1835) and *S. curvatus* are two morphologically similar species, the temporal ranges of which overlap in the upper Cenomanian. During this temporal overlap, the characteristics of one species intergrade into those of the other. One proposed solution has been to split *Squalicorax* species into a time-restricted morphological series, with *S. curvatus* existing in the Cenomanian and *S. falcatus* found in Turonian and Santonian deposits (Cappetta and Case, 1999). Shimada and Cicimurri (2006) refined these time frames to middle–upper Cenomanian for *S. curvatus* and upper Cenomanian–Santonian for *S. falcatus*. The lectotype of *S. falcatus* from the Turonian chalks of England does not appear to conform to *S. falcatus* of North America (Siverson et al., 2007). This observation has led some researchers to consider the fossil teeth described as *S. falcatus* from the Western Interior Seaway as being *S. curvatus*. There is continued debate as to the validity of *S. curvatus* as a species (Siverson et al., 2007), with some considering *S. curvatus* to be a synonym of *S. baharijensis* (Stromer, 1927) (Shimada et al., 2006) and others favoring retaining *S. curvatus* as a valid species while further exploring its relationship with *S. baharijensis* (Underwood and Cumbaa, 2010).

Results

Existing studies exploring the ultrastructure of *Ptychodus* enameloid have examined the tooth surface or sections, but not both. A comprehensive understanding of the ultrastructure of the dental enameloid of any taxon requires information gained by a combination of sectional and surface views (Enault et al., 2015) combined with magnifications sufficient to clearly see enameloid crystallites. This study compares the surface and sectional anatomy of a Pennsylvanian hybodontiform, the Cretaceous lamniform shark *Squalicorax curvatus*, and *Ptychodus* sp. to gain insight into the evolutionary lineage of *Ptychodus*.

Single-crystallite enameloid (SCE) of a hybodontiform.—The depth of the hybodontiform enameloid is about 600 μm from surface to the main body of dentine (Fig. 4.1). Channels for odontoblast processes and/or collagen fibers persist throughout the enameloid (Fig. 4.2). The structure of the enameloid is not surprisingly composed entirely of SCE at the surface of the tooth, midlevel, and at the enameloid-dentine junction (EDJ; Fig. 4.3, 4.4, 4.6). The individual crystallites of this SCE measure about 0.12 μm wide and about 0.8 μm. Tubules of orthodentine reach nearly to the surface of the enameloid. The denteons are approximately 75 μm in width with a central canal that is approximately 30 μm in diameter (Fig. 4.5). Tubules for odontoblast processes emanate from the central canal and provide entry into the enameloid. The base dentine is composed of osteodentine.

Triple-layered enameloid (TLE) of the neoselachian Squalicorax curvatus.—Prior to acid etching, small crystalline mineral material filled the spaces between apatite crystallites to such an extent that the surface of the enameloid was nearly featureless (Fig. 5.1). Following a one-minute treatment with 10% HCl, the crystallite structure of the SLE was apparent on the surface as a thin layer deposited on top of the PBE (Fig. 5.2). Individual enameloid crystallites in *S. curvatus* are about 0.1 μm in diameter and about 2 μm in length. Sectioned samples show the SLE to be about 2 μm in depth, with a relatively sharp boundary existing between SLE and the underlying PBE.

The PBE is visible by surface etching following 3 min of 10% HCl treatment (Fig. 5.3–5.6). These parallel bundles run from the base to the apex of the main and side cusps of the tooth. These bundles change direction as they near the serrations, turning so that they are oriented from the base to the apex of the serration (Fig. 5.3). In surface views, these bundles branch occasionally and unite with neighboring bundles, forming a mesh-like network of parallel bundles. In section, two populations of parallel bundles are apparent: longitudinal/axial bundles and radial bundles arising from the enameloid-dentine junction (EDJ) oriented orthogonally to the axials that terminate at the enameloid surface (Fig. 1).

The TBE is reliably visible only in sectioned teeth. This layer is composed of fibers of crystallites that interweave with each other and then transition to an inner network of single enameloid crystallites at the EDJ (Fig. 6.1–6.6). In *S. curvatus*, the TBE reaches the greatest level of development in the vicinity of the cusp apex and the serrations. The TBE thins out to less than 10 μm across most of the lingual and labial faces of the crown and comprises less than 10% of the enameloid thickness. Near the vertical midline of the *S. curvatus* tooth, the TBE is indistinguishable, except for scattered enameloid crystals (Fig. 6.5).

A relatively sharp boundary exists between the dentine and enameloid in *S. curvatus* (Fig. 6.1, 6.2). The crown dentine of *S. curvatus* is composed of osteodentine, and denteons are

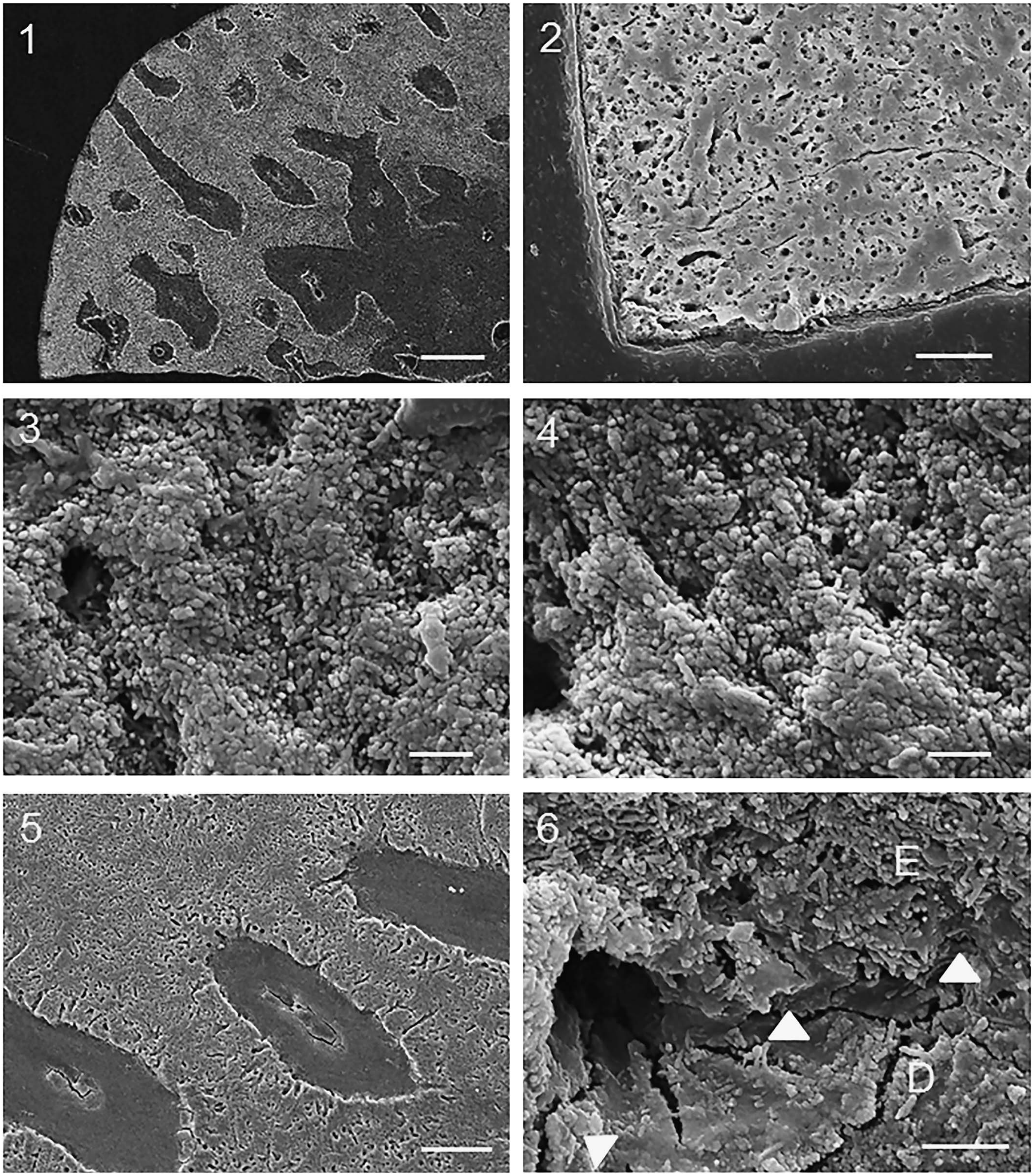

Figure 4. Enameloid ultrastructure of Pennsylvanian hybodontiform tooth sections (PUPC.2015.05.01). Scanning electron micrographs: (**1**) overview of sectioned tooth; (**2**) view of enameloid surface; (**3**) single crystallite enameloid of the tooth surface; (**4**) single crystallite enameloid of the middle of the tooth surface; (**5**) dentinal islands in enameloid; (**6**) single crystallite enameloid of the enameloid-dentine junction, indicated by arrows. Arrows indicate junction between the enameloid and dentine. E = enameloid; D = dentine. (**1**) Scale bar = 200 µm; (**2**) scale bar = 10 µm; (**3, 4, 6**) scale bars = 1 µm; (**5**) scale bar = 50 µm.

somewhat visible throughout the dentine, especially in cross section. The central cavity of the *S. curvatus* denteon is 25–30 µm. Concentric growth rings are visible, as are dentinal tubules, which appear to enter the enameloid (Fig. 6.2, 6.6).

Ptychodus *shiny-layered enameloid (SLE)*.—Prior to acid treatments, individual crystallites were not distinguishable on the surface of *Ptychodus* teeth (Fig. 7.1, 7.3, 7.5). Bumps on the ridges of *Ptychodus* samples provide just slightly more relief

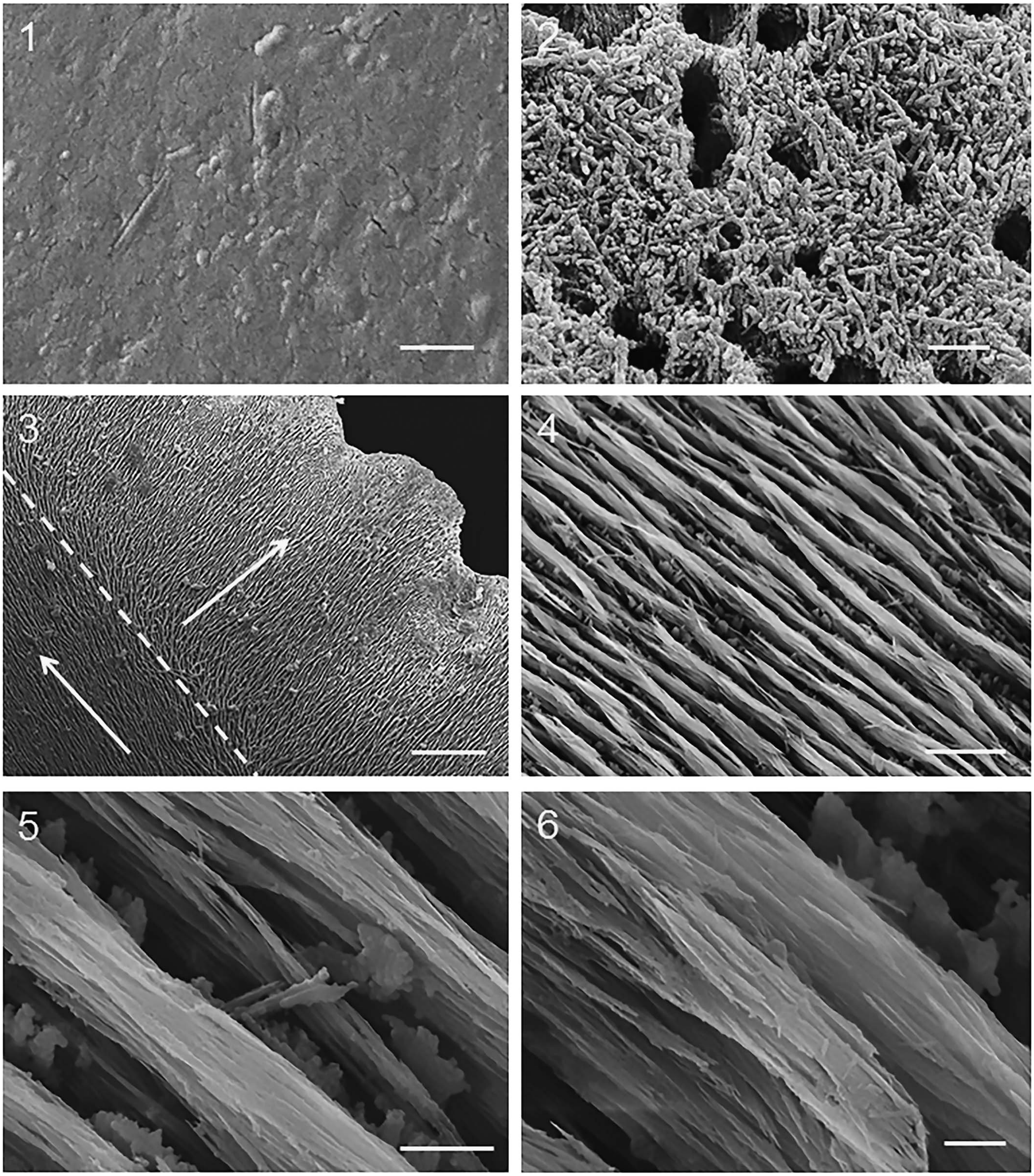

Figure 5. Single enameloid crystallites of the shiny-layered enameloid and parallel-bundled enameloid of *Squalicorax curvatus* teeth. Scanning electron micrographs: (**1**) surface of tooth PUPC 2015.06.01 before acid treatment; (**2**) surface of tooth PUPC 2015.06.02 treated with 10% HCl for 1 min showing single enameloid crystallites; (**3–6**) surface of tooth PUPC 2015.06.03 treated with 10% HCl for 3 min, showing parallel-bundled enameloid crystals. Dotted line in (**3**) shows the boundary between the apical parallel bundles and the parallel bundles of the serrations; arrows show direction of main parallel bundles. (**1, 2, 6**) Scale bars = 1 μm; (**3**) scale bar = 100 μm; (**4**) scale bar = 50 μm; (**5**) scale bar = 5 μm.

than was present on the surface of *S. curvatus*. Following a one-minute treatment with 10% HCl, the crystallite structure of the SLE was apparent on the tooth surface of *Ptychodus* sp. (Fig. 7.2, 7.4, 7.6). The crystallites show no preferential orientation in the SLE, and this layer varies from 2 to 5 μm thick. Individual crystallites are about 0.4 μm × 5–10 μm.

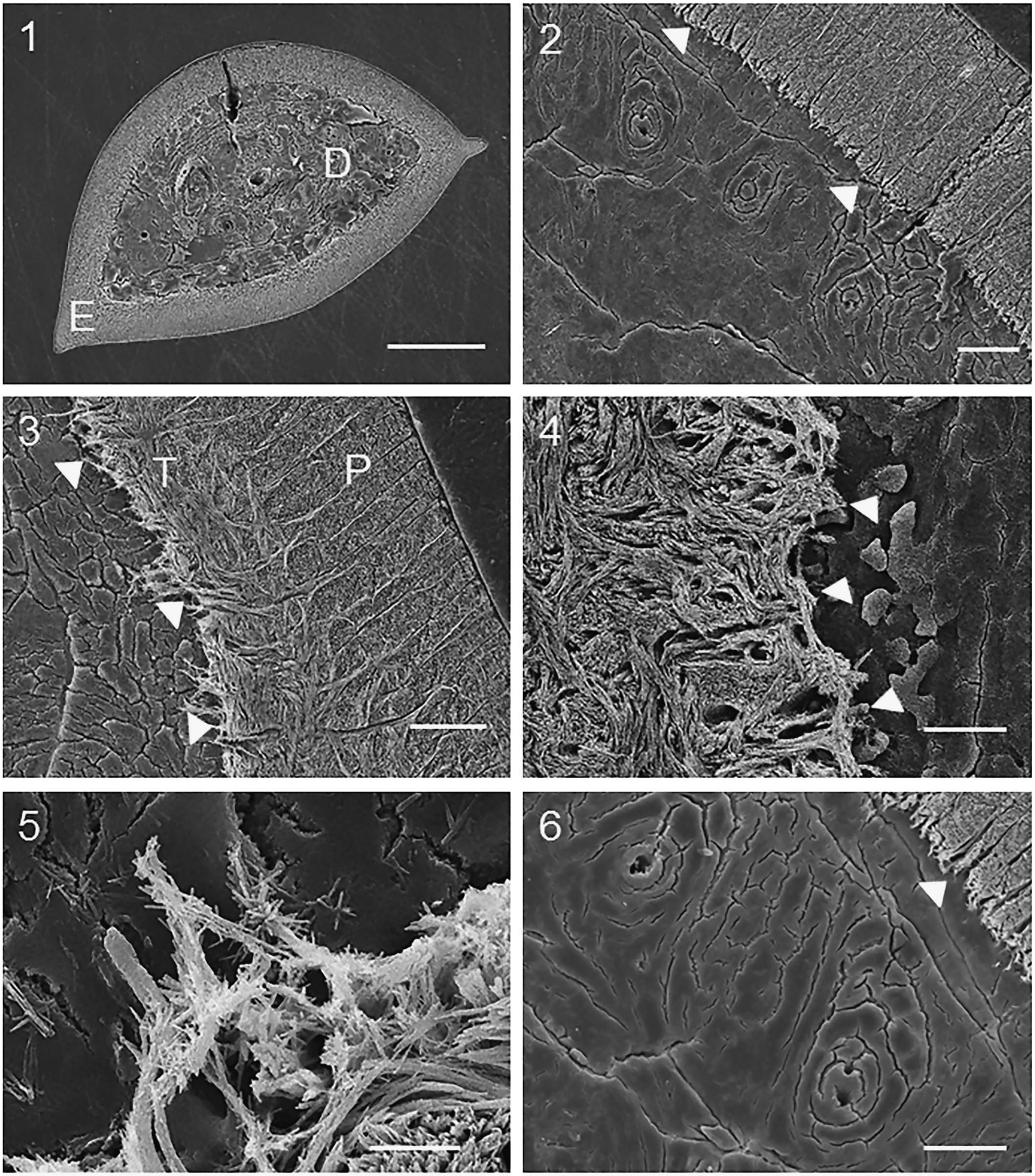

Figure 6. Tangled-bundled enameloid and dentine of *Squalicorax curvatus*. Scanning electron micrographs of sectioned tooth PUPC 2015.07.01: (**1**) cross section of *S. curvatus* tooth main cusp; (**2**) enameloid and osteodentine; (**3**) tangled-bundled enameloid between the dentine and parallel-bundled fibers; (**4**) tangled-bundled fibers (left) near the enameloid-dentine junction; (**5**) detail of the indistinct enameloid-dentine junction; (**6**) detail of dentine showing two osteons of the osteodentine. Arrows point to enameloid-dentine junction. E = enameloid; D = dentine; T = tangled-bundled enameloid; P = parallel-bundled enameloid. (**1**) Scale bar = 500 µm; (**2, 3, 6**) scale bars = 50 µm; (**4**) scale bar = 20 µm; (**5**) scale bar = 5 µm.

Ptychodus *parallel-bundled enameloid (PBE)*.—After three minutes of acid etching, the SLE was digested sufficiently to allow parallel rows of enameloid fibers to be visualized on the tooth surface (Fig. 8.1–8.6). This PBE is oriented orthogonally to the long axis of the enameloid ridges on the surface of the tooth and runs parallel to the long axis of the furrow

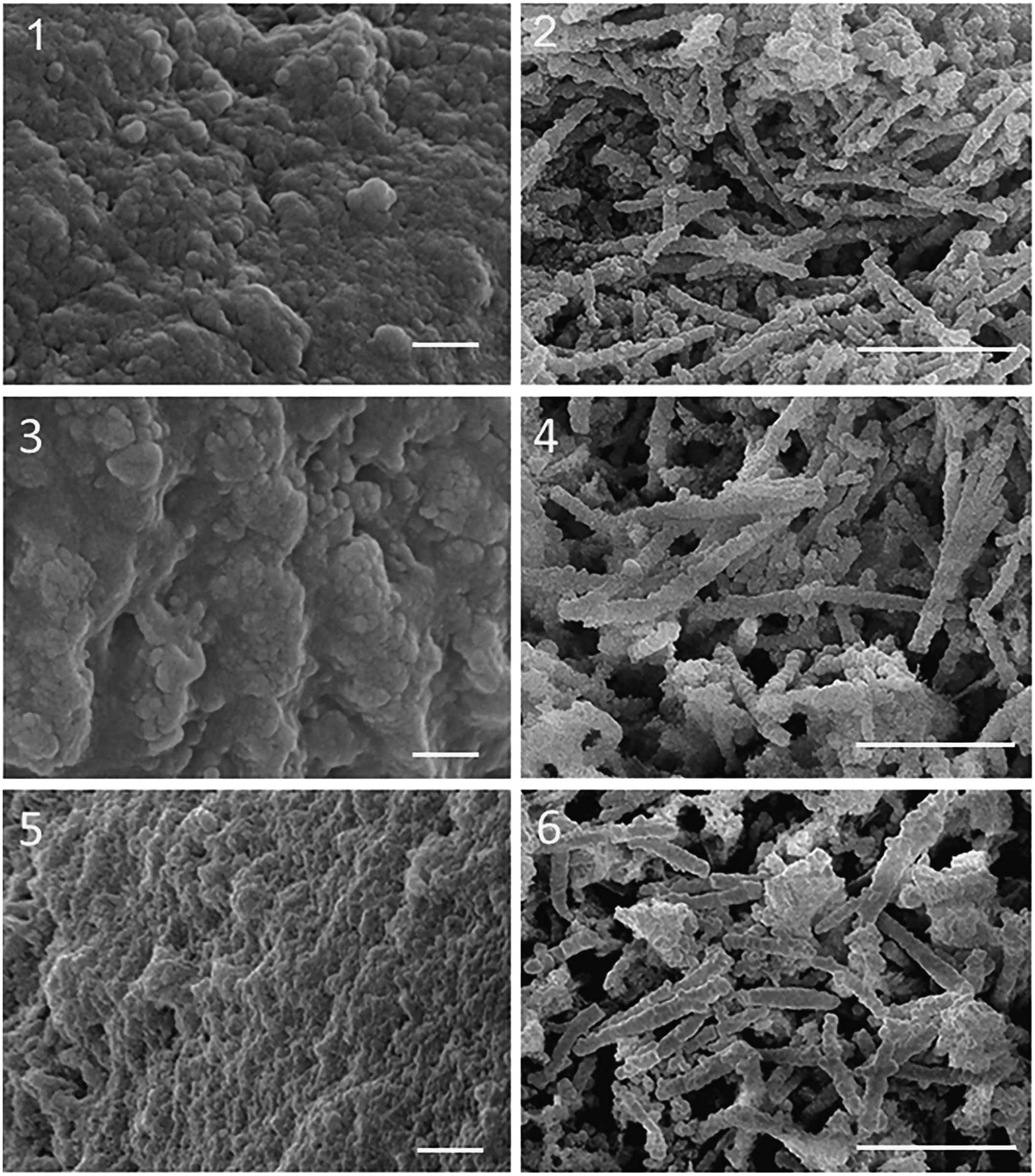

Figure 7. Single enameloid crystallites of the shiny-layered enameloid of *Ptychodus* teeth. Secondary electron images: (**1, 3, 5**) surface of *Ptychodus* teeth prior to acid treatment; (**2, 4, 6**) surface of *Ptychodus* teeth treated with 10% HCl for 1 min showing single enameloid crystallites; (**1**) PUPC 2015.08.01; (**2**) PUPC 2015.08.02; (**3**) PUPC 2015.08.03; (**4**) PUPC 2015.08.04; (**5**) PUPC 2015.08.05; (**6**) PUPC 2015.08.06. (**1, 3, 5**) Scale bars = 1 μm; (**2, 4, 6**) scale bars = 5 μm.

between ridges in *Ptychodus* (Fig. 8.5). In section, the PBE of *Ptychodus* is composed of perpendicular axial and radial fiber bundles (Figs. 9.1–9.6, 10.1–10.6). Axial bundles are oriented from the base to the apex of the crown and turn into serrations and ridges, running from the base to the apex of these structures. Both populations of these fibers are packaged

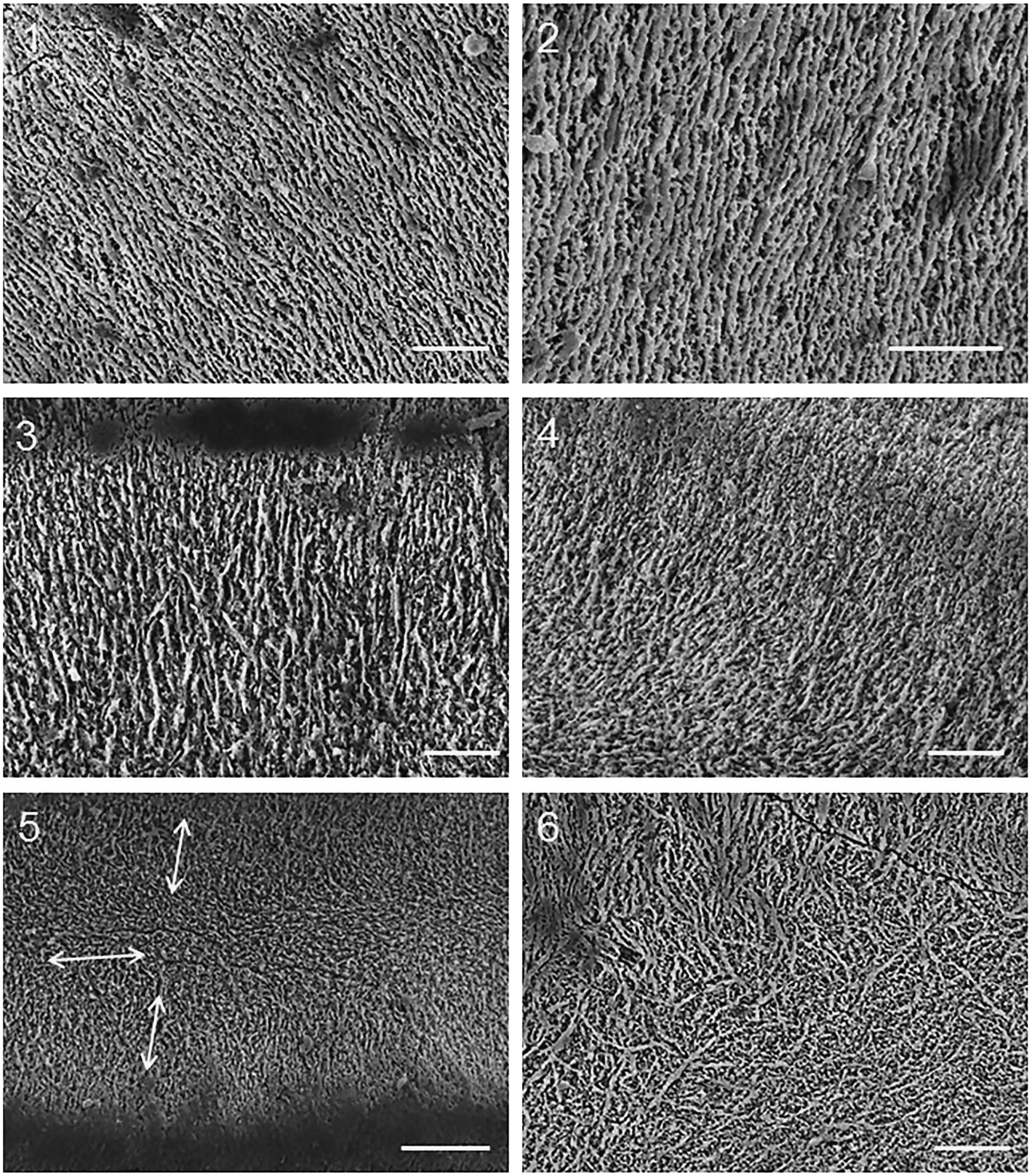

Figure 8. Surface views of the parallel-bundled enameloid *Ptychodus* teeth. Secondary electron images. (**1, 2**) Parallel bundles of enameloid on a transverse ridge of PUPC 2015.09.03. (**3–6**) Parallel bundles of enameloid between transverse ridges of PUPC 2015.09.02: (**3**) parallel bundles of enameloid on a transverse ridge of PUPC 2015.09.02 with base of ridge at bottom and apex of ridge at the top of the image; (**4**) parallel bundles of enameloid on a transverse ridge of PUPC 2015.09.02 with base of the ridge at bottom left and apex of the ridge at top right of the image; (**5**) parallel bundles of enameloid between transverse ridges, top of ridges at top and bottom of image and trough running from left to right in middle of image, arrows indicate orientation of bundles; (**6**) parallel bundles at junction of two ridges. (**1, 3, 4, 6**) Scale bars = 20 µm; (**2**) scale bar = 10 µm; (**5**) scale bar = 50 µm.

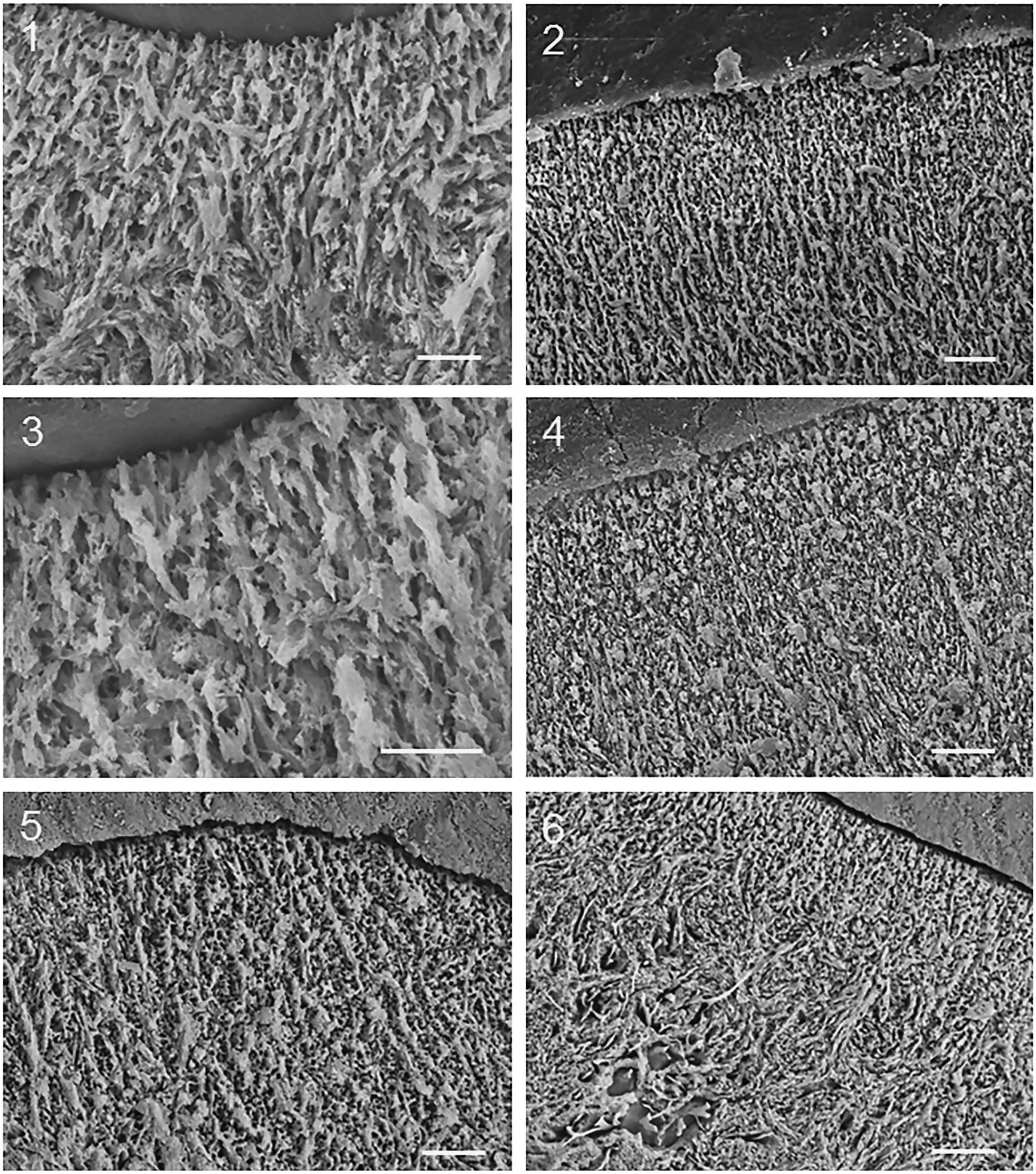

Figure 9. Parallel-bundled enameloid in sectioned *Ptychodus* sp. teeth. All secondary electron images: (**1, 3**) longitudinal section of PUPC 2015.11.01; (**2**) longitudinal section of PUPC 2015.10.01; (**4**) cross section of PUPC 2015.12.02; (**5**) longitudinal section of PUPC 2015.11.01; (**6**) cross section of PUPC 2015.17.01. Scale bars = 20 µm.

into large bundles in *Ptychodus* (Fig. 10.1–10.6) Bundled enameloid crystallites are best distinguished in the area of the crown containing transverse ridges. The enameloid of the tooth in the marginal areas tends to be composed of haphazardly oriented crystallites.

Ptychodus *tangled-bundled enameloid (TBE)*.—The TBE was reliably visible only in sectioned teeth after five to 10 seconds of 10% HCl etching (Fig. 11.1–11.6). The thickest layer of *Ptychodus* enameloid is the TBE, comprising 50%–80% of the enameloid thickness, depending on location within the crown.

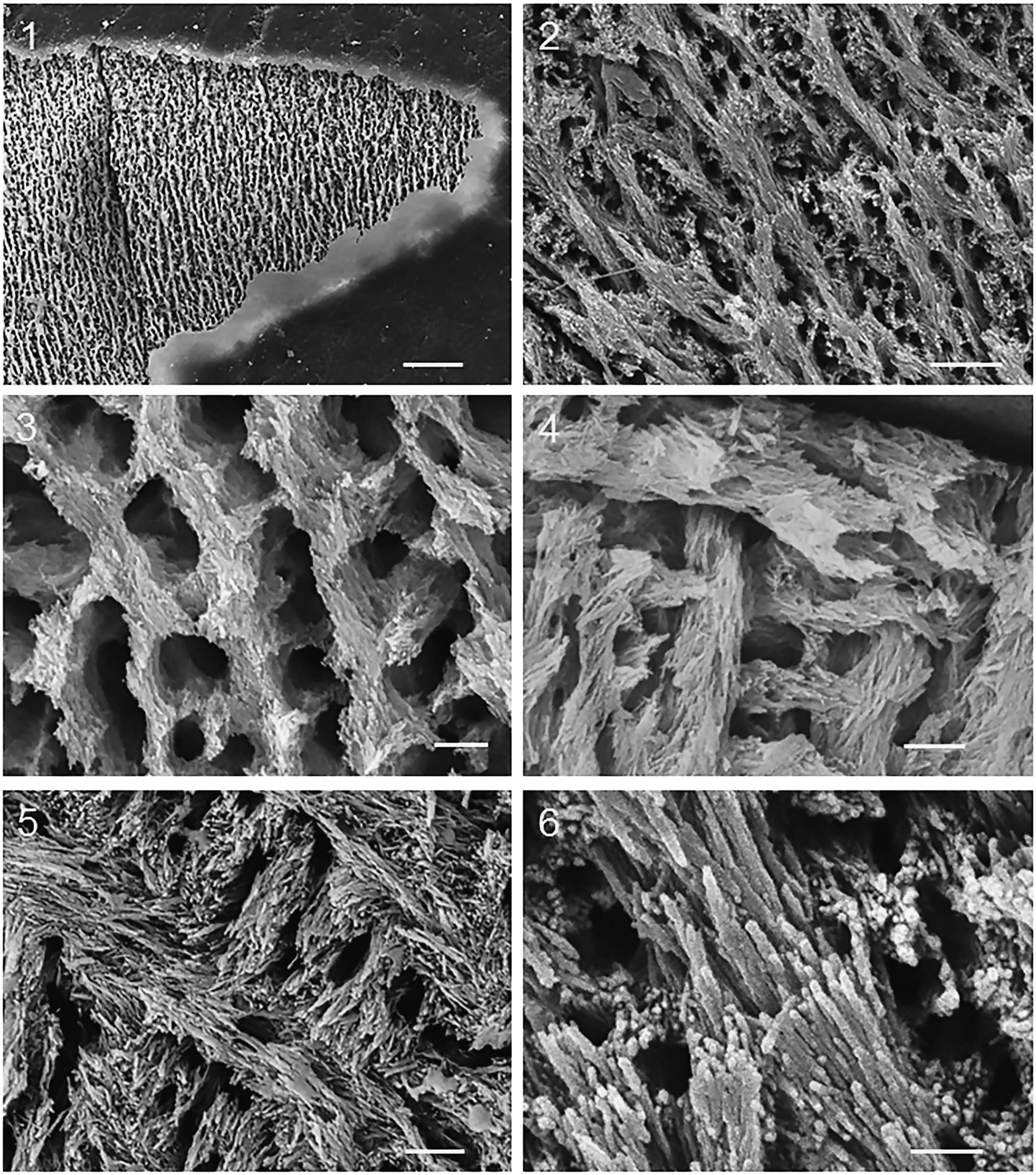

Figure 10. Bundling of enameloid crystallites in parallel-bundled enameloid in sectioned *Ptychodus* sp. teeth. (**1, 2, 6**) Secondary electron images; (**3–5**) backscattered electron images. (**1**) Parallel bundles of enameloid in longitudinal section of PUPC 2015.10.01; (**2**) same as (**1**), showing crystallites within parallel bundles; (**3**) cross section of PUPC 2015.12.02 showing perpendicular bundles of enameloid; (**4**) cross section of PUPC 2015.11.02 showing perpendicular bundles of enameloid; (**5**) parallel-bundled enameloid crystals in a cross section of PUPC 2015.10.02; (**6**) same as (**1**), showing bundling of crystallites in detail. (**1**) Scale bar = 20 µm; (**2–4**) scale bars = 5 µm; (**5**) scale bar = 2 µm; (**6**) scale bar = 1 µm.

The pathway taken by the bundled enameloid is heavily influenced by the presence of dentinal tubules, which intrude into the enameloid in the TBE (Fig. 11.3–11.5). As the enameloid-dentine junction is encountered, the bundled enameloid transitions back into a single crystallite enameloid (Fig. 11.5, 11.6).

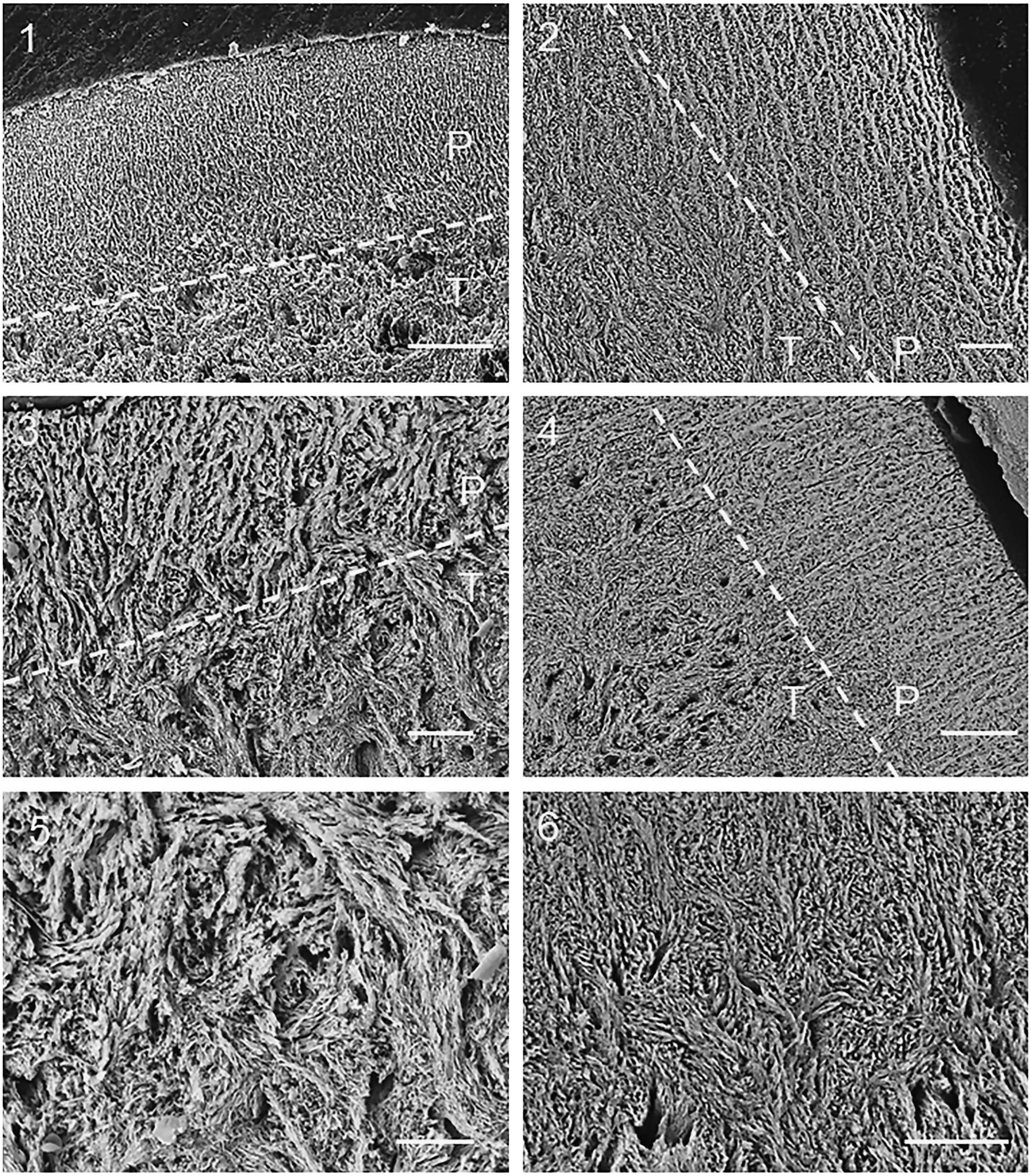

Figure 11. Tangled-bundled enameloid in sectioned *Ptychodus* sp. teeth. (**1, 2, 6**) Secondary electron images; (**3–5**) backscattered electron images. (**1**) Tangled-bundled enameloid in a longitudinal section of PUPC 2015.10.01; (**2**) tangled-bundled enameloid in a cross section of PUPC 2015.10.02; (**3**) tangled-bundled enameloid in a longitudinal section of PUPC 2015.11.01; (**4**) tangled-bundled enameloid in a longitudinal section of PUPC 2015.12.01; (**5**) detail of tangled-bundled enameloid of PUPC 2015.11.01; (**6**) detail of tangled-bundled enameloid of PUPC 2015.10.02. P = parallel-bundled enameloid; T = tangled-bundled enameloid; dashed line indicates the approximate boundary between PBE and TBE. (**1–4, 6**) Scale bar = 20 µm; (**5**) scale bar = 10 µm.

Ptychodus *dentine*.—*Ptychodus* teeth have a mixed dentinal structure (Figs. 12.1–12.4, 13.1–13.6). The roots are composed of osteodentine with numerous cavities for blood vessels (Fig. 12.3–12.4). The basal crown dentine is also composed of osteodentine as high as the top of the lingual groove and then transitions to orthodentine apically (Fig. 12.2). The orthodentine is organized

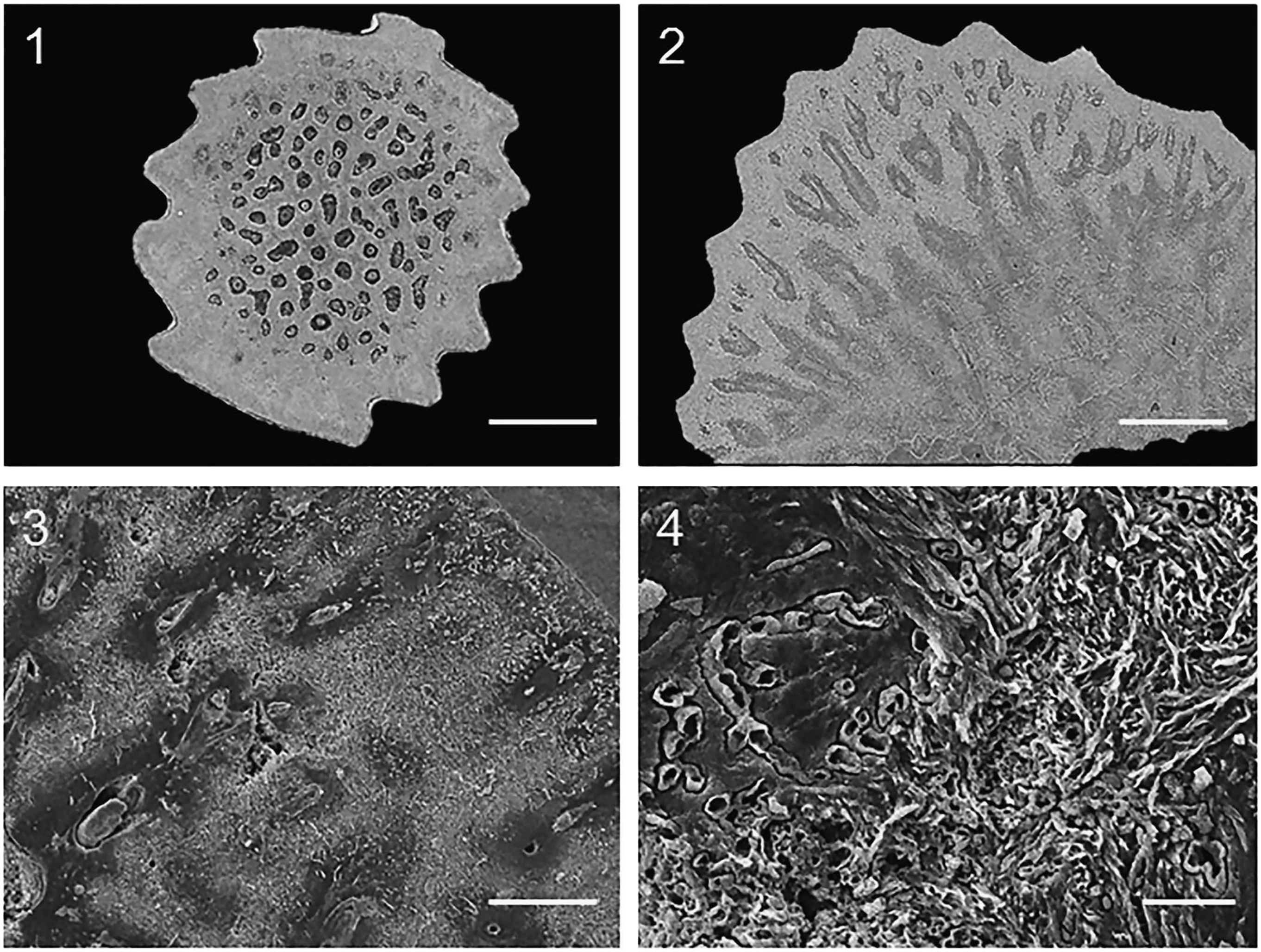

Figure 12. Overview of *Ptychodus* sp. crown and root dentine. Scanning electron micrographs: (**1**) cross section of crown of PUPC 2015.10.02; (**2**) longitudinal section of crown PUPC 2015.10.01; (**3, 4**) cross-sectional anatomy of tooth root of PUPC 2015.14.1. (**1, 2**) Scale bars = 500 µm; (**3**) scale bar = 200 µm; (**4**) scale bar = 20 µm.

as a plicidentine (Goto, 1991) between the enameloid and osteodentine (Fig. 13.1, 13.2). Columns of dentine extend into the enameloid. The denteons are about 100 µm across, with a central cavity that is about 30 µm in diameter. Casts of odontoblast processes are present, as are dentinal tubules conducting these processes into the enameloid (Fig. 13.3, 13.4). The enameloid at the enameloid-dentinal junction is composed of single crystallites that are randomly oriented (Fig. 13.5, 13.6).

Reconciling reports of single-crystallite enameloid in Ptychodus.—The presence of SCE in *Ptychodus* teeth has been noted in several reports (Cuny, 2008; Cappetta, 2012; Enault et al., 2015). In these experiments, a *Ptychodus* sp. tooth was immersed in 10% HCl for 23 minutes, 35 seconds (Enault et al., 2015) up to 34 minutes (Cuny, 2008). To replicate and assess this treatment, a *Ptychodus* sp. tooth was treated with 10% HCl for 23 min, 35 seconds. This produced a highly eroded tooth enameloid (Fig. 14.1–14.6) with visible patches of dentine containing odontoblast casts (Fig. 14.7, 14.8). Most of the surface ornamentation, with the exception of the most prominent ridges, was obliterated. Examination at high magnification (x1,000) showed the remaining enameloid to be single crystallite in structure (Fig. 14.9, 14.10).

Discussion

The taxonomic position of genus *Ptychodus* has proven to be enigmatic since the discovery of the first teeth (Everhart, 2013). The first descriptions of *Ptychodus* teeth assign them as potentially being palate bones of teleost fish (e.g., Hawkins, 1819; Conybeare and Phillips, 1822; Morton, 1834). Mantell (1822) noted that these teeth seemed to form a pavement dentition in the upper and lower jaw. Agassiz (1835) assigned the generic name *Ptychodus* to these teeth after the wrinkled appearance of the enameloid. Some 180 years later, several species have been described, including some from specimens that have associated or articulated dental sets (e.g., Williston, 1900; Woodward, 1904; MacLeod, 1982; Williamson et al., 1991; Shimada et al., 2009; Cappetta, 2012). Similarities to the pavement dentition of durophagous rays led Woodward (1887) to place *Ptychodus* within the Myliobatidae, a view that was accepted throughout much of the twentieth century but has since fallen out of favor. The two currently favored hypotheses for

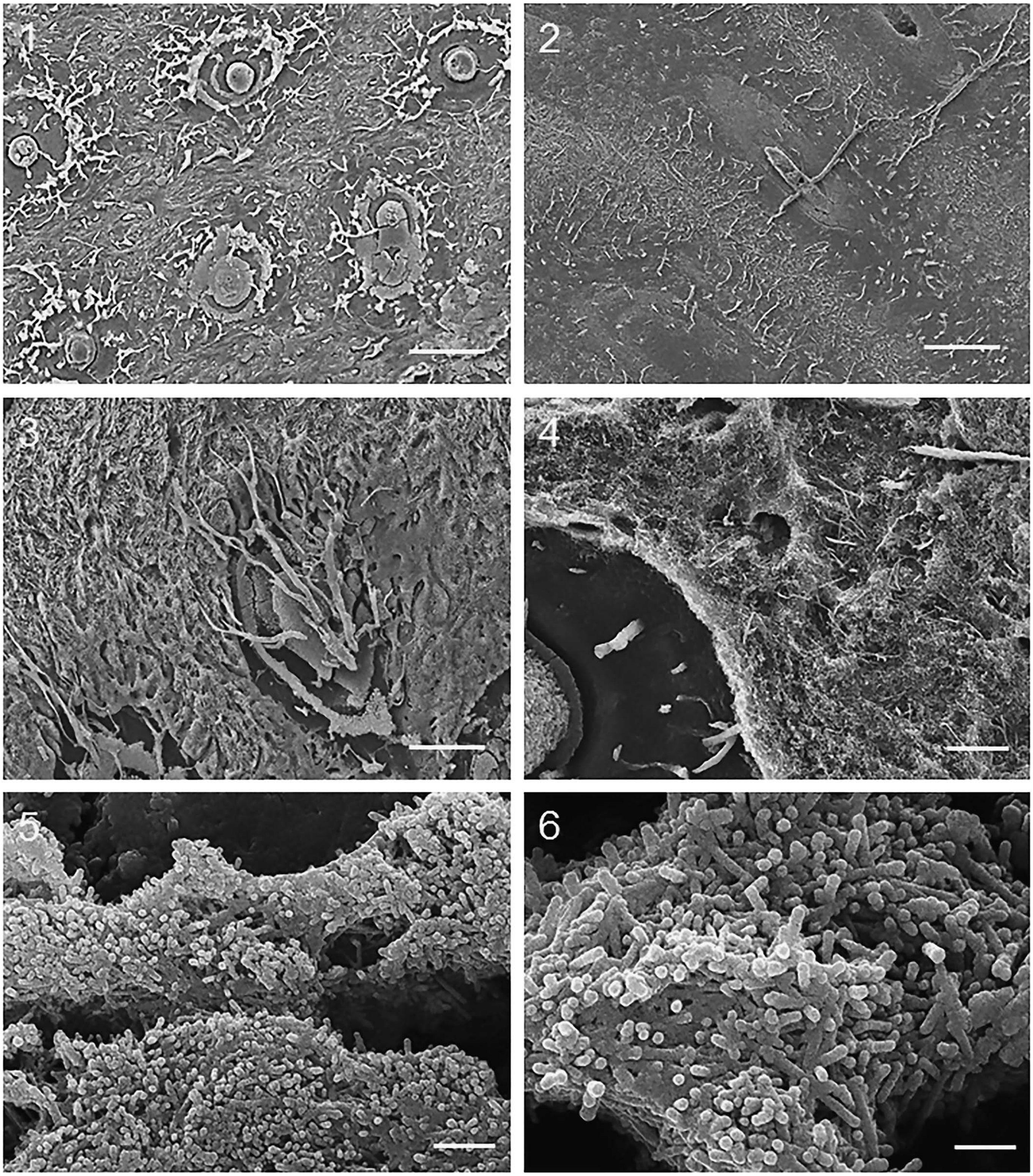

Figure 13. Crown dentine of *Ptychodus* sp. Scanning electron micrographs: (**1**) plicidentine in cross section of PUPC 2015.10.02; (**2**) plicidentine in longitudinal section of PUPC 2015.10.01; (**3**) dentinal island in enameloid of PUPC 2015.10.01; (**4**) dentinal island in enameloid of PUPC 2015.12.02; (**5, 6**) single enameloid crystallites adjacent to dentinal islands in enameloid of PUPC 2015.13.02. (**1, 3**) Scale bars = 50 µm; (**2**) scale bar = 100 µm; (**4**) scale bar = 10 µm; (**5**) scale bar = 2 µm; (**6**) scale bar = 1 µm.

classification of this genus are as follows: (1) *Ptychodus* belongs in the primitive shark order Hybodontiformes, mainly because of tooth structure; (2) *Ptychodus* is a highly specialized neoselachian, evidenced in features of scattered skeletal material (Cappetta, 2012).

Dental characteristics.—The hybodont affinity of *Ptychodus* is justified largely on macroscopic similarities in tooth anatomy (e.g., Patterson, 1966; Maisey, 1975, 1982; Brito and Janvier, 2002; Maisey et al., 2004; Hamm, 2015). Both have an

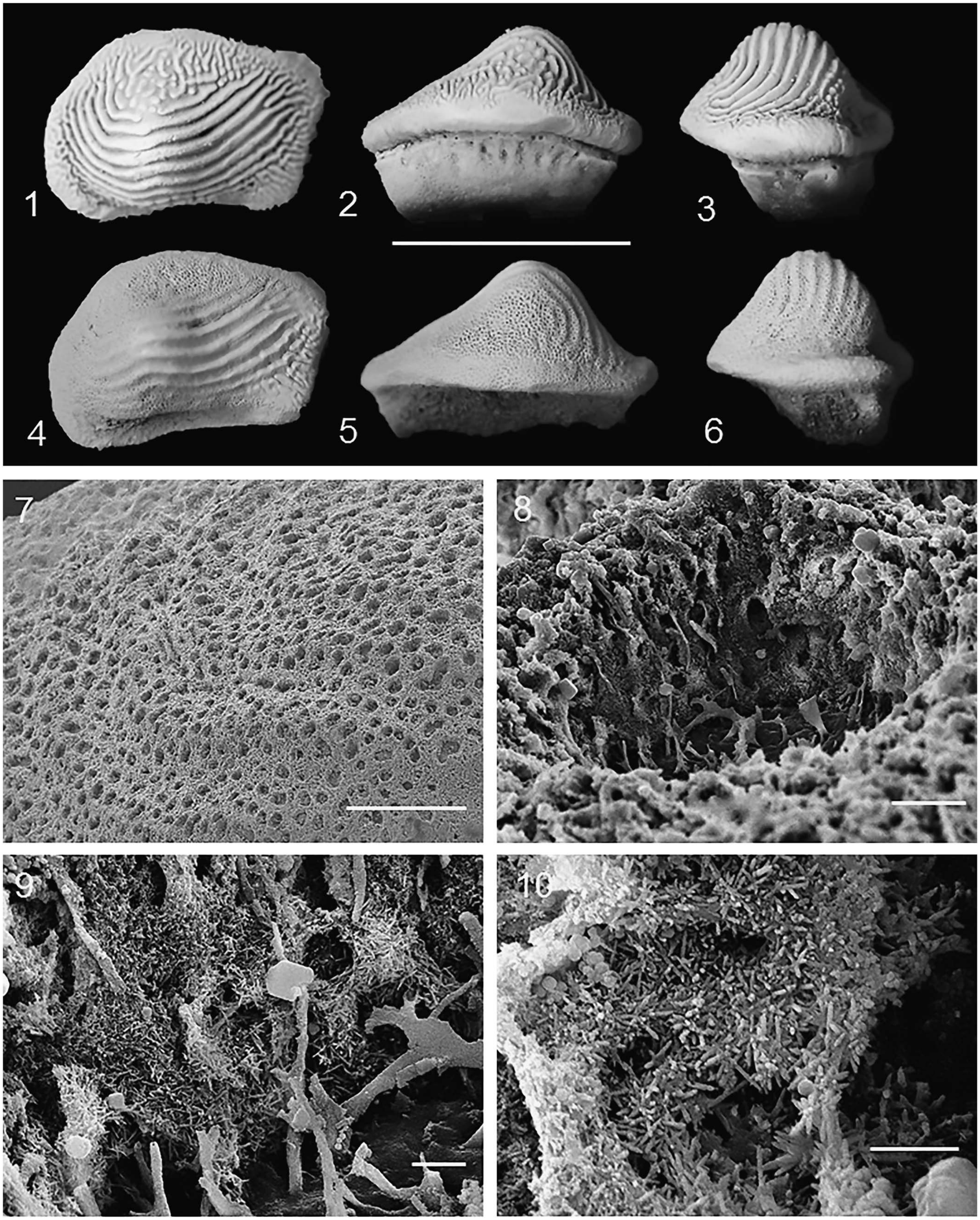

Figure 14. Effects of long acid exposures on enameloid structure of a *Ptychodus* sp. tooth. (**1–6**) Photomicrographs; (**7–10**) scanning electron micrographs. (**1–3**) *Ptychodus* tooth (PUPC 2015.16.01) prior to digestion with 10% HCl; (**4–6**) *Ptychodus* tooth following 23 min 35 sec digestion with 10% HCl; (**7**) surface view of acid digested tooth; holes in enameloid are exposed denteons; (**8**) detail of exposed denteon; (**9, 10**) randomly oriented single enameloid crystallites exposed by acid treatment; (**1, 4**) occlusal view; (**2, 5**) labial view; (**3, 6**) lateral view. (**1–6**) Scale bar = 1 cm; (**7**) scale bar = 500 µm; (**8**) scale bar = 20 µm; (**9, 10**) scale bars = 5 µm.

Table 1. Comparison of selected dental and skeletal characteristics of Mesozoic hybodonts and *Ptychodus* (based on Rees and Underwood, 2002; Hamm, 2015).

Character	Mesozoic Hybodonts	*Ptychodus*
Heterodonty	Monognathic	Dignathic
Dentition type	Cutting/grasping/crushing	Crushing
Crown type	Low and wide to gracile	Low and wide to high and narrow
Occlusal crest	Low to moderate	Well developed
Crown ornamentation	Weakly ridged	Strongly ridged
Labial protuberance	Strong	Well developed
Lingual sulcus	Weak	Well developed
Marginal ornamentation	Weak	Numerous reticulating folds and tubercles
Crown-root junction	Crown larger	Crown larger
Root vascularization	Anaulacorhizous	Anaulacorhizous
Root shape	Square to rectangular, flat	Rectangular, bilobed
Foramina at crown-root junction	Single row	Irregularly spaced, single row
Tooth enameloid	Single crystallite	Triple layered
Dorsal fin spines	Present	Absent
Cephalic spines	Present	Absent
Calcified vertebrae	Absent	Present
Pectoral fin	Aplesodic	Plesodic

anaulacorhizous tooth root, with numerous foramina penetrating the face of the root without evidence of a nutrient groove. The shape of the *Ptychodus* tooth root is rectangular, as are those of many hybodonts. Both have a massive crown that tends to overlap the roots. The nutrient foramina tend to form a single row at the crown-root junction in hybodonts and an irregularly spaced single row in *Ptychodus*. Both tooth types have noticeable labial protuberances. The *Ptychodus* tooth crown is of the crushing type, which is the primitive state in hybodonts and is evidenced in several species throughout the history of the lineage.

Despite these similarities, many dental differences exist between hybodonts and *Ptychodus* (Table 1). Hybodonts tend to show monognathic heterodonty, while *Ptychodus* exhibits dignathic heterodonty. The right and left palatoquadrates and Meckel's cartilages of *Ptychodus* exhibit symphysial fusion, unlike those of hybodonts. The occlusal crest on hybodont teeth is low to moderate, while that of *Ptychodus* teeth is well developed. A lingual sulcus that accommodates the labial protuberance of the tooth crown forming a peg and socket joint is well developed in *Ptychodus* but weak in hybodonts. The crown ornamentation is more strongly ridged in *Ptychodus* than in hybodonts. Marginal area ornamentation is likewise more extensively developed in *Ptychodus* than in hybodonts and is composed of numerous reticulating folds and tubercles, as compared to hybodonts.

Tooth architecture and histology alone provide very little insight into the taxonomic placement of different sharks (Cappetta, 2012). Similarities in tooth structure often result from convergent evolution, driven as much by selective pressures exerted by diet as by evolutionary relatedness. The fact that dentinal tubules penetrate into the enameloid of both the hybodont *Asteracanthus* and *Ptychodus* (Bendix-Almgreen, 1983; Cuny, 2008; Enault et al., 2015) is cited as evidence of familial relationship between Hybodontiformes and *Ptychodus* (Cuny, 2008; Enault et al., 2015), although it seems just as likely to be a convergent trait that favors durophagy.

The extensively bundled enameloid of *Ptychodus* is important in distinguishing this genus from the hybodonts. Hybodont enameloid is composed of randomly oriented fluroapatite crystallites, with some possibly exhibiting very short bundles of crystallites (Enault et al., 2015). Ptychodontid enameloid is demonstrated in the current study to have a triple-layered enameloid (TLE) structure characteristic of selachimorph neoselachians. Bundled enameloid is not limited to selachimorphs as parallel-bundled enameloid (PBE) has recently been imaged in the teeth of the Permian ctenacanthiform *Neosaivodus flagstaffensis* Hodnett et al. (2012) and two unnamed species of Cretaceous (Valanginian) cladodontomorph sharks (Guinot et al., 2013). The survival of cladodontomorph sharks into the Cretaceous is postulated to have been due to habitat expansion of these sharks into deepwater refugia (Guinot et al., 2013). Convergent development of PBE in cladodontomorphs potentially gave the tooth added strength to change from grasping-clutching predators of fish to being able to pierce the bodies of pelagic hard-shelled organisms. Although PBE is apparently not unique to the selachimorph sharks, the triple-layered enameloid is, and that of *Ptychodus* allows differentiation from the hybodonts.

Skeletal characteristics.—Very few complete skeletons of Mesozoic hybodonts exist, and only relatively scattered skeletal remains of *Ptychodus* have been found. In concert with dental structure, skeletal material is instructive in classifying these sharks. Hybodonts characteristically possess one or two pairs of cephalic spines and a fin spine anterior to the dorsal fins that have a groove and sizeable denticles on the posterior margin of the fin spine (e.g., Maisey, 1982; Rees and Underwood, 2002; Rees, 2008; Hamm, 2015). No cephalic hooks or fin spines that could belong to *Ptychodus* have been found, despite the abundance *of Ptychodus* teeth in Cretaceous chalk deposits of the United States and England (Cappetta, 2012). A putative dorsal fin associated with *P. mortoni* (Agassiz, 1843) teeth (in KUVP 59061) shows no evidence of an anterior fin spine, nor does it display an articulation for a fin spine (Hamm, 2008). Pectoral fin remains of KUVP 59061 indicate that *Ptychodus* had plesodic pectoral fins, while those of Mesozoic hybodonts are aplesodic (Coates and Gess, 2007).

Calcified vertebral centra, an autapomorphy of neoselachian sharks, have been associated with several *Ptychodus* dentitions (e.g., Woodward, 1889; Canavari, 1916; Stewart, 1980; Everhart and Caggiano, 2004; Shimada et al., 2009; Hamm, 2010). The centra are round and resemble those of lamniform sharks, which suggest that *Ptychodus* had the classic fusiform body shape of a pelagic predator. Although some of these centra lay quite close to dentition and jaw cartilages (e.g., Shimada et al., 2009), some workers point out that a direct connection between skull elements and centra is lacking (e.g., Mutter et al., 2005; Cappetta, 2012; Enault et al., 2015). Judging from preservation state of the remains, proximity of the teeth and vertebrae, taphonomic features of the specimens, depositional setting, and apparent decomposition rates of sharks and bony fish in the Western Interior Seaway (Hattin, 1975; Elder, 1987; Cumbaa et al., 2006; Landman and Klofak, 2012; Schmeisser McKean and Gillette, 2015), it is likely that the associated assemblage of teeth and vertebrae come from a single individual. A formal possibility exists that a line of large hybodonts may have developed calcified centra in parallel with the neoselachians (Cappetta, 2012; Enault et al., 2015), but no such examples have been discovered. Placoid scales from *Ptychodus* also have shapes that are characteristic of a fast-swimming shark (Hamm, 2010).

Does Ptychodus *have an SCE or a TLE?*—Previous studies have presented limited views of the enameloid of *Ptychodus*. The ultrastructure of ptychodontid enameloid has become a major point of discussion in attempts to describe *Ptychodus* as a neoselachian or hybodont (Cuny, 2008; Hamm, 2008, 2010; Cappetta, 2012; Enault et al., 2015). The single most compelling reason to place *Ptychodus* among the hybodonts is the assertion that the teeth of this genus have an enameloid composed of SCE (Cuny, 2008; Cappetta, 2012; Enault et al., 2015), a primitive elasmobranch character. This assertion is based primarily on a single figure (Cuny, 2008, fig. 1a, 1b), which is replicated in a later paper (Enault et al., 2015, fig. 2k, 2l). This figure shows an electron micrograph of a tooth of *Ptychodus* sp. from Craie du Blanc-Nez, France, etched in 10% HCl for 34 min (Cuny, 2008) or 23 min 35 sec (Enault et al., 2015). The enameloid of this tooth is degraded to such an extent by prolonged acid treatments that most surface features are barely recognizable, and at least 100 µm of enameloid has likely been removed judging from observations of enameloid thickness and location of dentine (Fig. 11). In the figures by Cuny (2008) and Enault et al. (2015), many holes appear in the enameloid that are actually exposed denteons, which are also seen in Figure 14.7. The relatively thin SCE (2–5 µm), the PBE (30–60 µm), and much of the TBE must be removed to give this appearance, providing an inaccurate evaluation of the microstructure of the enameloid. What have been interpreted in previous studies as an SCE in *Ptychodus* (Cuny, 2008; Enault et al., 2015) are actually what remains of the TBE after extremely long incubation with HCl. Our results show that the enameloid crystallites at the dentinal border are randomly oriented, as are the crystallites remaining after 23 minutes of HCl treatment. Much shorter treatments in the present study reveal the SLE (1 min) and PBE (3 min) on the surface of whole teeth (Figs. 7, 8) and sectioned teeth exhibit a complex pattern of bundling in the form of parallel bundles and tangled-fibered bundles (Figs. 9, 10, 11).

Examination of the dental structure of a Pennsylvanian hybodontiform shark (Fig. 4) provides additional information about the crystallite bundling in *Ptychodus*. It is formally possible that the very presence of denteons and odontoblast processes in the enameloid could generate a pattern that mimics bundling. This is especially true of the TBE, which could be crystallites falling into file around these structures. The fact that the enameloid of this hybodontiform retains an obvious SCE even in the presence of denteons indicates that true bundling of crystallites is occurring in *Ptychodus*. The use of dentine to provide reinforcement against the stresses generated on teeth by a durophagous diet arose as early as the Carboniferous sharks and likely arose by convergence several times during shark evolution, as it is also seen in Mesozoic hybodonts like *Asteracanthus* (Bendix-Almgreen, 1983; Enault et al., 2015).

The TLE found in these *Ptychodus* sp. teeth is consistent with previous observations of *Ptychodus* enameloid in the literature. Bendix-Almgreen (1983, fig. 6A, 6B) examined sections of *P. latissimus* teeth from England that show a noticeable PBE and TBE. What appears to be the SLE forms a thin layer above the PBE, although the magnification of the specimen is not sufficient to make that determination certain. David (1996, 1999, pls. 2, 3, 5, 10, 11) also identified the TLE structure in *P. decurrens* (Agassiz, 1839) (Lincoln Limestone Member, Greenhorn Limestone Formation, Russell County, Kansas) and *P. mortoni* (Smoky Hills Member, Niobrara Chalk Formation, Scott County, Kansas). SEM examination of the teeth of more ptychodontid shark species should help to elucidate in-family evolutionary relationships (Hamm, 2008).

Implications for Ptychodus *ecology.*—The similarity in the ultrastructure and function of *Ptychodus* and *S. curvatus* teeth is striking. The PBE is oriented along the long axis of the crown (base to apex of the crown) and turn into the serrations so that they are oriented from the base to the apex of the serration in *S. curvatus* (Fig. 6.3), which is the pattern reported by David (1999) and Andreev (2010). Between ridges, the PBE of *Ptychodus* is oriented from the lateral margins of the tooth to the crown of the tooth. The PBE fibers turn at the ridges and run from the base to the apex of the ridge (Fig. 8). The apexes of the serrations in *S. curvatus* and ridges in *Ptychodus* are both covered in a dense material that is resistant to degradation by acid. These characteristics point to the functional similarity of the serrations of cutting type dentitions and the ridges of the crushing type dentition of *Ptychodus*. The apex and serrations of the pointed *S. curvatus* tooth serve to concentrate bite force to grasp prey and then easily tear into flesh. Well-developed axial bundles in these structures would spread pressure loads over the surface of the tooth to minimize bending and breakage, making it a logical evolutionary adaptation. The apex of the *Ptychodus* tooth could act as a pressure point for grasping and breaking/piercing thinly shelled invertebrates, while the transverse ridges probably would help serve as secondary pressure points used to apply three-point bending pressure (such as in a nutcracker) for cracking thicker shells while spreading the pressure load over a larger surface area of the tooth.

The parallel bundles of *Ptychodus* enameloid are oriented both normally and parallel to the crown surface of the tooth. Unlike *S. curvatus*, in which the radial bundles are much thinner than the axial bundles, both sets of bundles are of approximately the same thickness in *Ptychodus*. This is suggestive of stress being placed onto the tooth in not only a vertical, but also a horizontal plane, which would be present in an organism chewing with a grinding motion. The TBE likewise provides resistance to twisting motions that would be present when breaking up thicker shells. These teeth belong to medium- to high-crowned species of *Ptychodus*. The shape of the tooth and reinforcement of the longitudinal ridges may have allowed *Ptychodus* to not only eat hard-shelled organisms but also grasp softer-bodied prey, supporting a generalist predation strategy rather than a highly specialized diet restricted to relatively few species in the Western Interior Seaway. An added advantage is that several species of *Ptychodus* could occupy the same geographic space at the same time without necessarily occupying the same ecological niche (Hamm, 2008; Myers and Lieberman, 2011) or competing with other predators (e.g., other sharks and large marine reptiles).

Consideration of the dental and skeletal structure of *Ptychodus* allows construction of a picture of this shark as a highly specialized, fast-swimming, dietary generalist capable of occupying various depths of the ocean. The pavement dentition allows for the exploitation of beds of inoceramid bivalves in the benthos of the Western Interior Seaway as shown by attritional wear on *Ptychodus* teeth and bite marks consistent with *Ptychodus* teeth on *Inoceramus* shells (Kauffman, 1972, 1977). *Ptychodus* likely scooped up mud containing small, thin-shelled clams and their epibionts, leaving the much larger clams behind (Everhart, 2005). Benthic neoselachians have vertebral centra that are dorsolaterally compressed, yielding a flattened body (Compagno, 1977). The round, calcified centra of *Ptychodus* are indicators of a fusiform body, complemented by dermal denticles characteristic of fast-swimming sharks, meaning that *Ptychodus* also likely fed on free-swimming organisms such as small fish and cephalopods (e.g., ammonites and belemnoids). Modern durophagous batoids that inhabit continental shelf and epipelagic environments do not depend solely on benthic organisms, consuming free-swimming cephalopods as well as fish (Ebert and Stehmann, 2013).

Conclusions

Triple-layered enameloid is accepted as a dental synapomorphy of selachimorph sharks, and its presence in *Ptychodus* indicates that this shark should be classified in the Neoselachii and is not a hybodont. This study indicates that possession of a TLE is probably characteristic for *Ptychodus*. The complexity of *Ptychodus* enameloid may indicate that these sharks had a diet that was much broader than that of the stereotypical shell-crushing shark. Not only is *Ptychodus* enameloid much different from that of hybodonts, but when comparing several characteristics seen in hybodonts and *Ptychodus* simultaneously, it becomes apparent that there are more differences than similarities between these two groups of sharks.

Acknowledgments

The authors thank the family of the late Alan H. Kamb for their generous donation of portions of his collections to the Park University Geology Collection, including the teeth used in this study, and M. Everhart, T. Cook, A. Murray, B. Pratt, and an anonymous reviewer for comments that greatly improved the quality of the manuscript. This work was supported in part by grants from the Park University Faculty Development Endowment Fund that supplied reference materials (BLH) and specimen storage cabinets (SAH and BLH), and monetary support was received from the John and Hazel Shafer Memorial Foundation.

References

Agassiz, L., 1833–1844, Recherches sur les Poissons Fossiles [5 volumes]: Neuchâtel, Imprimerie de Petitpierre, 1420 p.

Andreev, P.S., 2010, Enameloid microstructure of the serrated cutting edges in certain fossil carcharinifrom and lamniform sharks: Microscopy Research and Technique, v. 73, p. 704–713.

Andreev, P.S., and Cuny, G., 2012, New Triassic stem selachimorphs (Chondrichthyes, Elasmobranchii) and their bearing on the evolution of dental enameloid in Neoselachii: Journal of Vertebrate Paleontology, v. 32, p. 255–266.

Bendix-Almgreen, S.E., 1983, *Carcharodon megalodon* from the Upper Miocene of Denmark, with comments on elasmobranch tooth enameloid: Coronoïn: Bulletin of the Geological Society of Denmark, v. 32, p. 1–32.

Berg, L.S., 1937, A classification of fish-like vertebrates: Bulletin de l'Académie des Sciences de l'URSS, v. 1937, p. 1277–1280 [in Russian with English summary].

Bonaparte, C.L., 1838, Selachorum tabula analytica: Nuovi Annali della Scienze Naturali, Bologna, v. 1, p. 195–214.

Brito, P.M., and Janvier, P., 2002, A ptychodontid (Chondrichthyes, Elasmobranchii) from the Upper Cretaceous of South America: Geodiversitas, v. 24, p. 785–790.

Canavari, M., 1916, Descrizione di um notevole esemplare di *Ptychodus* Agassiz trovato nel calcare bianco della Creta superior di Gallio nei Sette Comuni (Veneto): Palaeontographica Italica, v. 22, p. 35–102.

Cappetta, H., 2012, Chondrichthyes—Mesozoic and Cenozoic Elasmobranchii: Teeth. Handbook of Paleoichthyology, v. 3E: Munich, Verlag Dr. Friedrich Pfeil, 512 p.

Cappetta, H., and Case, G.R., 1999, Additions aux faunes de sélachiens du Crétaché du Texas (Albian supérieur-Campanien): Paleo Ichthyologica, v. 9, p. 5–111.

Casier, E.N., 1947, Constitution et évolution de la racine dentaire des Euselachii. II-Etude comparative des types: Bruxelles Bull. Mus. r. Hist. nat. Belg, v. 23, no. 4, p. 1–32.

Coates, M.I., and Gess, R.W., 2007, A new reconstruction of *Onychoselache traquairi*, comments on early chondrichthyan pectoral girdles and hybodontiform phylogeny: Palaeontology, v. 50, p. 1421–1446.

Compagno, L.J.V., 1977, Phyletic relationships of living sharks and rays: American Zoologist, v. 17, p. 303–322.

Conybeare, W.D., and Phillips, W., 1822, Outlines of the Geology of England and Wales. Part I, London, William Phillips, 477 p.

Cumbaa, S.L., Schröder-Adams, C., Day, R.G., and Phillips, A.J., 2006, Cenomanian bonebed faunas from the northeastern margin, Western Interior Seaway, Canada: New Mexico Museum of Natural History and Science Bulletin, v. 35, p. 139–155.

Cuny, G., 2008, Mesozoic hybodont sharks from Asia and their relationships to the genus *Ptychodus*: Acta Geologica Polonica, v. 58, p. 211–216.

Cuny, G., and Risnes, S., 2005, The enameloid microstructure of the teeth of synechodontiform sharks (Chondrichthyes: Neoselachii): PalArch Foundation Journal of Vertebrate Palaeontology, v. 3, p. 8–19.

Cuny, G., Srisuk, P., Khamha, S., Suteethorn, V., and Tong, H., 2009, A new elasmobranch fauna from the middle Jurassic of southern Thailand: Geological Society, London, Special Publications, v. 315, p. 97–113.

David, M.L., 1996, Dental histology of *Ptychodus* and its implications in the phylogeny of the Ptychodontidae: Journal of Vertebrate Paleontology, v. 16, no. 3 (supplement), p. 30A.

David, M.L., 1999, A histological and mechanical description of *Ptychodus* [M.S. thesis]: Hays, Fort Hays State University, 44 p.

Dick, J.R.F., 1978, On the Carboniferous shark *Tristychius arcuatus* from Scotland: Transactions of the Royal Society of Edinburgh, v. 70, no. 4, p. 63–109.

Dick, J.R.F., and Maisey, J.G., 1980, The Scottish lower Carboniferous shark *Onychoselache traquairi*: Palaeontology, v. 23, p. 363–374.

Douady, C., Dosay, M., Shivji, M.S., and Stanhope, M.J., 2003, Molecular phylogenetic evidence refuting the hypothesis of Batoidea (rays and skates) as derived sharks: Molecular Phylogenetics and Evolution, v. 26, p. 215–221.

Ebert, D.A., and Stehmann, M.F.W., 2013, Sharks, batoids and chimaeras of the North Atlantic, Rome, FAO Species Catalogue for Fishery Purposes, no. 7, 523 p.

Elder, W.P., 1987, The paleoecology of Cenomanian-Turonian (Cretaceous) boundary extinctions at Black Mesa, Arizona: PALAIOS, v. 2, no. 1, p. 24–40.

Enault, S., Cappetta, H., and Adnet, S., 2013, Simplification of the enameloid microstructure of large stingrays (Chondricthyes: Myliobatiformes): A functional approach: Zoological Journal of the Linnean Society, v. 169, p. 144–155.

Enault, S., Guinot, G., Koot, M.B., and Cuny, G., 2015, Chondrichthyan tooth enameloid: Past, present, and future: Zoological Journal of the Linnean Society, v. 174, p. 549–570.

Enax, J., Janus, A.M., Raabe, D., Epple, M., and Fabritius, H.-O., 2014, Ultrastructural organization and micromechanical properties of shark tooth enameloid: Acta Biomateriala, v. 10, p. 3959–3968.

Everhart, M.J., 2005, The Oceans of Kansas: A Natural History of the Western Interior Sea, Bloomington, Indiana University Press, 344 p.

Everhart, M.J., 2013, “The Palate Bones of a Fish?”—The first specimen of *Ptychodus mortoni* (Chondrichthyes; Elasmobranchii) from Alabama: Bulletin of the Alabama Museum of Natural History, v. 31, p. 98–104.

Everhart, M.J., and Caggiano, T., 2004, An associated dentition and calcified vertebral centra of the Late Cretaceous elasmobranch, *Ptychodus anonymus* Williston 1900: Paludicola, no. 4, 125–136.

Gallardo, C., Shimada, K., and Schumacher, B.A., 2013, A new Late Cretaceous marine vertebrate assemblage from the Lincoln Limestone Member of the Greenhorn Limestone in southeastern Colorado: Kansas Academy of Science, Transactions, v. 115, no. 3/4, p. 107–116.

Gillis, J.A., and Donoghue, P.C.J., 2007, The homology and phylogeny of chondrichthyan tooth enameloid: Journal of Morphology, v. 268, p. 33–49.

Ginter, M., Hampe, O., and Duffin, C., 2010, Chondrichthyes—Paleozoic Elasmobranchii: Teeth. Handbook of Paleoichthyology, v. 3D: Munich, Verlag Dr. Friedrich Pfeil, 168 p.

Goto, M., 1991, Evolutionary trends of the tooth structure in Chondrichthyes, *in* Suga, S., and Nakahara, H., eds., Mechanisms and Phylogeny of Mineralization in Biological Systems: Biomineralization ’90: Tokyo, Springer-Verlag, p. 447–452.

Guinot, G., and Cappetta, H., 2011, Enameloid microstructure of some Cretaceous Hexanchiformes and Synechodontiformes (Chondrichthyes: Neoselachii): New structures and systematic implications: Microscopy Research and Technique, v. 74, p. 196–205.

Guinot, G., Adnet, S., Cavin, L., and Cappetta, H., 2013, Cretaceous stem chondrichthyans survived the end-Permian mass extinction: Nature Communications, doi:10.1038/ncomms3669.

Hamm, S.A., 2008, Systematic, stratigraphic, geographic and paleoecological distribution of the Late Cretaceous shark genus *Ptychodus* within the Western Interior Seaway [M.S. thesis]: Dallas, University of Texas-Dallas, 434 p.

Hamm, S.A., 2010, The Late Cretaceous shark, *Ptychodus rugosus*, (Ptychodontidae) in the Western Interior Sea: Kansas Academy of Science, Transactions, v. 113, no. 1/2, p. 44–55.

Hamm, S.A., 2015, *Paraptychodus washitaensis* n. gen. et n. sp., of Ptychodontid shark from the Albian of Texas, USA: Cretaceous Research, v. 54, p. 60–67.

Hansen, M.C., 1986, Microscopic chondrichthyan remains from Pennsylvanian marine rocks of Ohio and adjacent areas [Ph.D. dissertation], Columbus, The Ohio State University, 536 p.

Hattin, D.E., 1975, Stratigraphy and depositional environment of Greenhorn Limestone (Upper Cretaceous) of Kansas: Bulletin of Kansas Geological Survey, no. 209, 128 p.

Hawkins, A., 1819, Kingsbridge and Salcombe, with an Intermediate Estuary, Historically and Topographically Depicted, London, R. Southwood, 210 p.

Hay, O.P., 1902, Bibliography and catalogue of fossil Vertebrata of North America: United States Geological Survey Bulletin, v. 179, 868 p.

Hodnett, J.-P., Elliot, D.K., Olson, T.J., and Wittke, J.H., 2012, Ctenacanthiform sharks from the Permian Kaibab Formation, northern Arizona: Historical Biology, v. 24, p. 381–395.

Huxley, T.H., 1880, On the application of the laws of evolution to the arrangement of the Vertebrata and more particularly the Mammalia: Proceedings of the Zoological Society of London, v. 1880, p. 649–662.

Jaekel, O.M.J., 1898, Die Selachier aus dem oberen Muschelkalk Lothringens. Abhandteilung Geologische Spezialk: Elasass-Lothringen, Series 3, no. 4, p. 273–332.

Kauffman, E.G., 1972, *Ptychodus* predation upon a Cretaceous *Inoceramus*: Journal of Paleontology, v. 15, p. 439–444.

Kauffman, E.G., 1977, Geological and biological overview: Western Interior Cretaceous basin: The Mountain Geologist, v. 14, no. 3/4, p. 75–99.

Kauffman, E.G., Sageman, B.B., Kirkland, J.I., Elder, W.P., Harries, P.J., and Villamil, T., 1993, Molluscan biostratigraphy of the Cretaceous Western Interior Basin, North America, *in* Caldwell, W.G.E., and Kauffman, E.G., eds., Evolution of the Western Interior Basin: Geological Association of Canada, Special Paper no. 39, p. 397–434.

Landman, N.H., and Klofak, S.M., 2012, Anatomy of a concretion: Life, death and burial in the Western Interior Seaway: PALAIOS, v. 27, no. 10, p. 671–692.

Leidy, J., 1868, Notice of American species of *Ptychodus*: Proceedings of the Academy of Natural Sciences of Philadelphia, v. 20, p. 205–208.

Macleod, N., 1982, The first North American occurrence of the Late Cretaceous elasmobranch *Ptychodus rugosus*: Journal of Paleontology, v. 56, p. 403–409.

Maisey, J.G., 1975, The interrelationships of phalacanthous selachians: Neues Jahrbüch für Geologie and Paläontologie Monatschefte, v. 1975, no. 9, p. 553–567.

Maisey, J.G., 1982, The anatomy and interrelationships of Mesozoic hybodont sharks: American Museum Novitates, v. 2724, p. 1–48.

Maisey, J.G., Naylor, G.J.P., and Ward, D.J., 2004, Mesozoic elasmobranchs, neoselachian phylogeny, and the rise of modern neoselachian diversity, *in* Arratia, G., and Tintori, A., eds., Mesozoic Fishes 3—Systematics, Paleoenvironments and Biodiversity, Munich, Verlag Dr. Friedrich Pfeil, p. 17–56.

Mantell, G.A., 1822, Fossils of the South Downs, or, Illustrations of the geology of Sussex, London, Lupton Relfe, 320 p.

McKirahan, J., Goldstein, R.H., and Franseen, E.K., 2000, Sequence stratigraphy of the Lane-Island Creek Shales and the Farley Limestone in northeastern Kansas and geologic factors affecting the quality of limestone aggregates: Kansas Department of Transportation Report, no. K-TRAN: KU-97-1, p. 6–70.

Morton, S.G., 1834, Synopsis of the Organic Remains of the Cretaceous Group of the United States, Philadelphia, Key and Biddle, 89 p.

Mutter, R.J., Itturalde-Vinent, M., and Carmona, J.F., 2005, The first Mesozoic Caribbean shark is from the Turonian of Cuba: *Ptychodus cyclodontis* sp. nov. (?Neoselachii): Journal of Vertebrate Paleontology, v. 25, p. 976–978.

Myers, C.E., and Lieberman, B.S., 2011, Sharks that pass in the night: Using geographical information systems to investigate competition in the Western Interior Seaway: Proceedings of the Royal Academy of Sciences B, v. 278, p. 681–689.

Patterson, C., 1966, British Wealden sharks: Bulletin of the British Museum (Natural History) Geology, v. 11, p. 283–350.

Preuschoft, H., Reif, W.E., and Muller, W.H., 1974, Funktionsanpassungen in form und struktur an haifischzähnen: Zeitschrift für Anatomie und Entwicklungsgeschichte, v. 143, p. 315–344.

Rees, J., 2008, Interrelationships of Mesozoic hybodont sharks as indicated by dental morphology—preliminary results: Acta Geologica Polonica, v. 58, p. 217–221.

Rees, J., and Underwood, C.T., 2002, The status of the genus *Lissodus* Brough, 1935, and the position of the nominal *Lissodus* species within the Hybodontoidea (Selachii): Journal of Vertebrate Paleontology, v. 22, p. 471–478.

Reif, W., 1973, Morphologie und Skulptür der Haifisch-Zähnkronen: Neues Jahrbüch für Geologie and Paläontologie Abhandlungen, v. 143, p. 39–55.

Reif, W., 1977, Tooth enameloid as taxonomic criterion: 1. A new euselachian shark from the Rhaetic-Liassic boundary: Neues Jahrbüch für Geologie and Paläontologie Monatschefte, v. 1977, p. 565–576.

Rocco, L., Liguori, I., Costagliola, D., Morescalchi, M.A., Tintl, F., and Stingo, V., 2007, Molecular and karyological aspects of Batoidea (Chondrichthyes: Elasmobranchii) phylogeny: Gene, v. 389, p. 80–86.

Schmeisser McKean, R.L., and Gillette, D.D., 2015, Taphonomy of large marine vertebrates in the Upper Cretaceous (Cenomanian-Turonian) tropic shale of southern Utah: Cretaceous Research, v. 56, p. 278–292.

Schultze, H.-P., and Chorn, J., 1988, The Upper Pennsylvanian vertebrate fauna of Hamilton, Kansas, *in* Mapes, G., and Mapes, R.H., eds., Regional Geology and Paleontology of Upper Paleozoic Hamilton Quarry Area in Southeastern Kansas: Kansas Geological Survey Guidebook, no. 6, p. 147–154.

Shimada, K., and Cicimurri, D.J., 2006, The oldest record of the Late Cretaceous anacoracid shark *Squalicorax pristodontus* (Agassiz), from the Western Interior, with comments on *Squalicorax* phylogeny, *in* Lucas, S.G., and Sullivan, R.M., eds., Late Cretaceous Vertebrates from the Western Interior: New Mexico Museum of Natural History and Science Bulletin, no. 35, p. 177–184.

Shimada, K., Schumacher, B.A., Parkin, J.A., and Palermo, J.M., 2006, Fossil marine vertebrates from the Lowermost Greenhorn Limestone (Upper Cretaceous: Middle Cenomanian) in Southeastern Colorado: Journal of Paleontology, v. 80 (supplement to no. 2), Memoir 63.

Shimada, K., Rigby, C.J., and Kim, S.H., 2009, Partial skull of Late Cretaceous durophagous shark *Ptychodus occidentalis* (Elasmobranchii: Ptychodontidae), from Nebraska, U.S.A: Journal of Vertebrate Paleontology, v. 29, p. 336–349.

Siverson, M., Lindquist, J., and Kelly, L.S., 2007, Anacoracid sharks from the Albian (Lower Cretaceous) Pawpaw Shale of Texas: Palaeontology, v. 50, p. 939–950.

Stewart, J.D., 1980, Reevaluation of the phylogenetic position of the Ptychodontidae: Kansas Academy of Science, Transactions, v. 83, no. 3, p. 154.

Stewart, J.D., 1988, Paleoecology and the first West Coast record of the shark genus *Ptychodus*: Journal of Vertebrate Paleontology, v. 8, no. 3 (supplement) p. 27A.

Stromer, E., 1927, Prof. E. Stromers in den Wüsten Ägyptens. II. Wirbeltier-Reste der Baharije-Stufe (Unterstes Cenoman). 9. Die Plagiostomen mit einem Anhang über käno- und mesozoische Rückenflossenstacheln von Elasmobranchiern: Abhandlungen der Bayerischen Akademie der Wissenschaften, Mathematisch-naturwissenschaftliche Abteilung, Neue Funde, 31, p. 1–64.

Underwood, C.J., and Cumbaa, S.L., 2010, Chondrichthyans from a Cenomanian (Late Cretaceous) bonebed, Saskatchewan, Canada: Paleontology, v. 53, p. 903–944.

Whitenack, L.B., Simpkins, D.C. Jr., Motta, P.J., Hirai, M., and Kumar, A., 2010, Young's modulus and hardness of shark tooth biomaterials: Archives of Oral Biology, v. 55, p. 203–209.

Whitenack, L.B., Simpkins, D.C. Jr., and Motta, P.J., 2011, Biology meets engineering: The structural mechanics of fossil and extant shark teeth: Journal of Morphology, v. 272, p. 169–179.

Whitley, G.P., 1939, Taxonomic notes on sharks and rays: Australian Zoologist, v. 9, no. 3, p. 227–262.

Williamson, T.E., Kirkland, J.I., and Lucas, S.G., 1991, The Cretaceous elasmobranch Ptychodus decurrens Agassiz from North America: Geobios, v. 24, p. 595–599.

Williston, S.W., 1900, Some fish teeth from the Kansas Cretaceous: Kansas University Quarterly, v. 9, p. 27–42.

Winchell, C.J., Martin, A.P., and Mallat, J., 2004, Phylogeny of elasmobranchs based on LSU and SSU ribosomal RNA genes: Molecular Phylogenetics and Evolution, v. 31, p. 214–224.

Woodward, A.S., 1887, On the dentition and affinities of the selachian genus *Ptychodus* Agassiz: Quarterly Journal of the Geological Society, London, v. 43, p. 121–131.

Woodward, A.S., 1889, Catalogue of the Fossil Fishes in the British Museum, London, British Museum of Natural History, 474 p.

Woodward, A.S., 1904, The jaws of *Ptychodus* from the Chalk: Quarterly Journal of the Geological Society, London, v. 60, p. 133–135.

Zangerl, R., 1981, Chondrichthyes I: Paleozoic Elasmobranchii. Handbook of Paleoichthyology, v. 3A: Stuttgart, Gustav Fischer, 115 p.

Accepted 23 February 2016